Available online at www.sciencedirect.com
SCIENCE DIRECT®
Icarus 166 (2003) 248–270
ICARUS
www.elsevier.com/locate/icarus

Error statistics of asteroid optical astrometric observations

Mario Carpino,[a,*] Andrea Milani,[b] and Steven R. Chesley [c]

[a] *Osservatorio Astronomico di Brera, via Brera, 28, 20121 Milan, Italy*
[b] *Dipartimento di Matematica, Università di Pisa, Via Buonarroti, 2, 56127 Pisa, Italy*
[c] *Navigation & Mission Design Section, MS 301-150, Jet Propulsion Laboratory, Pasadena, CA 91109, USA*

Received 29 May 2001; revised 25 October 2002

Abstract

Astrometric uncertainty is a crucial component of the asteroid orbit determination process. However, in the absence of rigorous uncertainty information, only very crude weighting schemes are available to the orbit computer. This inevitably leads to a correspondingly crude characterization of the orbital uncertainty and in many cases to less accurate orbits. In this paper we describe a method for carefully assessing the statistical performance of the various observatories that have produced asteroid astrometry, with the ultimate goal of using this statistical characterization to improve asteroid orbit determination. We also include a detailed description of our previously unpublished automatic outlier rejection algorithm used in the orbit determination, which is an important component of the fitting process.

To start this study we have determined the best fitting orbits for the first 17,349 numbered asteroids and computed the corresponding O–C astrometric residuals for all observations used in the orbit fitting. We group the residuals into roughly homogeneous bins and compute the root mean square (RMS) error and bias in declination and right ascension for each bin. Results are tabulated for each of the 77 bins containing more than 3000 observations; this comprises roughly two thirds of the data, but only 2% of the bins. There are several interesting results, including substantial bias from several observatories, and some distinct non-Gaussian characteristics that are difficult to explain. Several limitations of our approach and possible future improvements are discussed.

The correlation of errors among observations taken closely together in time is in many cases an important issue that has rarely been considered. We have computed the mean correlation between observations with varying time separations and obtained empirical functions that model the results. This has been done for several observatories with very large data sets (the remainder has been lumped into a single mixed batch). These functions could be used for estimating correlation coefficients among different observations of the same observatory, supplying a new observation weighting scheme based upon an empirically tested observational error model.

Keywords: Asteroids; Data reduction techniques; Orbits

1. Introduction

When asteroid orbits are computed by fitting astrometric observations the result is not only a single *nominal solution*, but a *region of confidence* where the orbital elements are compatible with the observations. However, the definition of such a confidence region depends upon assumptions on the possible errors contained in the observations. Reliable information on the statistics of observational errors allows one to define a statistical model of the result in the space of orbital elements; this model in turn defines not only the confidence boundaries, but also the probabilities of finding the orbital elements within each boundary. Prom this probabilistic assessment of the initial conditions at some epoch it is possible to compute an analogous probabilistic assessment for every prediction based upon the future (and past) state of the asteroid, such as a predicted observation (Milani, 1999), a close approach (Milani and Valsecchi, 1999; Milani et al., 2000a), an orbit identification (Milani et al., 2000b), or an attribution of observations (Milani et al., 2001). Whenever the predictions have substantial uncertainty, either because the orbit is weakly determined by too few observations, the prediction is required with extreme precision, or the prediction is for a time remote from the observations, this probabilistic point of view should always replace the simple mention of the nominal prediction. Deterministic statements are superior to probabilistic ones only when they are reliable, otherwise they could be a source of confusion and even a waste of resources.

* Corresponding author.
E-mail address: carpino@brera.mi.astro.it (M. Carpino).

0019-1035/$ – see front matter
doi:10.1016/S0019-1035(03)00051-4

The statistical model of the observational errors cannot be decided on the basis of some theoretical argument only: an error model needs to be confirmed by empirical evidence. The observational errors are found by analyzing the residuals, after removing the sources of error not related to the observations (e.g., the orbital errors). We should not force the errors to be what we believe they should be: an a priori model cannot be reliable since a complete physical and statistical model of the observational procedure, including the astrometric reduction, would be too complicated and is certainly not available. In particular, the classical assumption (Gauss, 1809) that the observation errors are *normally distributed*, that is distributed according to a Gaussian probability density function, is not an axiom but should be an assumption to be tested against empirical evidence. This is even more true since there is no such thing as a unique Gaussian model, but there is a multidimensional space of Gaussian probability density functions, depending upon parameters values are not known a priori.

Thus we have set as our research goals the following tasks. First, we would like to test the hypothesis that there is a statistical model of the observational errors in asteroid astrometry, in particular a Gaussian model, which can be empirically confirmed by analyzing a large and representative set of residuals. Second, we would like to find the values of the parameters defining the most appropriate Gaussian distribution, in particular the standard deviations, biases and correlations, in such a way that the model best fits the reality of the observational process. Third, we would like to assess the impact of the use of such a nontrivial statistical model on the orbit determination, by comparing the results with those obtained with a naive error model and by measuring the improvements, if any, in the reliability of the predictions. This paper contains the results ob the first two tasks, while the work on the third one is ongoing.

A motivation for this work is the need to replace the simplistic error model that is implicitly assumed when the target function of the least-square orbit determinations is just the sum of squares of the residuals (with equal weights for all the observations) or maybe with weighting based upon crude assumptions. There are very good reasons to think that different observatories have very different accuracies, that there are systematic as well as random errors, and that the errors are not independent but correlated. The simplistic model was previously used mostly for lack of something better, rather than because it was credible. We intend to use the error models derived from this paper in a weighting scheme to be used for orbit determination.

This paper is organized as follows: in Section 2 we describe the preparation of a large set of astrometric residuals, which have been used for this statistical analysis; this includes an algorithm for outlier rejection that we have developed. In Section 3 we find the most suitable values of the root mean squares (RMS) and bias to be attached to a presumed Gaussian distribution of the observational errors. In Section 4 we find empirical correlation functions which correspond to the real behavior of the data, to be used to replace the simplistic assumption of uncorrelated observations. We conclude in Section 5 by discussing the internal consistency of the statistical model of the observation errors based upon the RMS, bias and correlations computed in this paper. Finally we indicate the work which remains to be done to fully achieve our goal: to firmly base the orbit determination algorithm on a more rigorous and reliable statistical model.

2. Observation residuals

We have prepared the residuals (observed minus computed values of right ascension and declination) to be analyzed by computing least-square solutions for a large set of orbits, applying a differential correction algorithm until convergence. Strictly speaking, the two steps of orbit determination and statistical analysis of the residuals are interdependent, since the statistical analysis is performed on the residuals generated by orbit determination and orbit determination uses the results of the statistical analysis for assigning weights to the observations and for performing outlier rejection. It is therefore necessary to adopt an iterative approach: as a starting point, we have used a simplistic model with no correlations, no bias and all residuals weighted according to a crude scheme. (We used weights corresponding to an assumed RMS of 1 arcsec for modern observations, 2 arcsec before 1950, and 3 arcsec before 1890.) The use of such a poor model affects the results in an uncertain way, with implications discussed in Section 5.

2.1. Data set

A reliable statistical study of observational error requires a large and homogeneous data set of residuals that can be interpreted as observational errors. Astrometric observations of asteroids observed only at a single opposition cannot be used for this purpose, because in a least-square fit of a short arc a large fraction of the observation error can be absorbed in the values of the fit parameters (orbital elements) and therefore does not show up in the residuals. For this reason we have used only the data for numbered asteroids, specifically, the data published by the Minor Planet Center with the monthly update of 19 September 2000, which contained 2,145,404 optical observations of 17,349 numbered asteroids (we are not counting, for this purpose, the radar observations).

2.2. Outlier dejection

The algorithm for differential corrections we have used in preparing the residuals data set includes an automatic outlier rejection scheme. This is necessary because in fact the data contain some observations with very large errors. These can arise from erroneous identifications, from mistakes in the astrometric reduction, from typographical errors and many

other human and machine failures. Such erroneous observations can corrupt the orbital solution; thus they must be removed. Having done this, we can assume that the nominal least-square orbit is the true one, at least to an accuracy much better than that given by any single observation. This implies that the residuals essentially contain only observation errors, but this chain of assumptions needs to be verified a posteriori.

In this section we carefully describe the algorithms we have used to reject the outliers in a fully automated way. The basic idea is to use the information supplied by the statistical analysis of the residuals (see Section 3) and discard as outliers all the observations for which the residual is too high. This approach entails forming a 2×2 residual covariance for each right ascension and declination pair. The covariance of the residual differs from the measurement covariance because some component of the residuals can be attributed to orbital error. By combining the measurement and orbital covariances one can determine if a particular residual violates some threshold of acceptability. From that, one can determine not only if an observation should be rejected, but also if a previously rejected observation should be recovered into the fit.

The following description of the automated outlier rejection method is important because it describes a critical part of the process by which we have obtained the residuals that form the basis of our statistical analysis. However, a detailed understanding of this method is not particularly relevant when considering the main results of this paper, namely a comprehensive analysis of the statistics of asteroid astrometric errors. We also recognize that such details may not be of interest to many readers and so we have structured the paper such that skipping to Section 2.5 or to Section 3 will not substantially detract from the presentation.

2.3. Theory of outlier rejection

The term χ^2 can be considered the generalization of the concept of *normalized squared residual* for vectorial stochastic variables $x \in \Re^n$ and is defined as

$$\chi^2 = (x - \bar{x})' W_x (x - \bar{x}),$$

where $\bar{x} = \mathcal{E}[x]$ is the *stochastic expectation value or stochastic average* (here indicated by the operator $\mathcal{E}[\cdot]$) of the stochastic variable x and W_x is the $n \times n$ weight matrix of x, equal to the inverse of its covariance matrix Γ_x:

$$W_x = \Gamma_x^{-1}.$$

The covariance matrix Γ_x is defined as the stochastic expectation value of the $n \times n$ matrix $(x - \bar{x})(x - \bar{x})'$:

$$\Gamma_x = \mathcal{E}\big[(x - \bar{x})(x - \bar{x})'\big].$$

In the case of a one-dimensional stochastic variable $x \in \Re$, Γ_x is simply the *variance* σ_x^2 and χ^2 reduces to the normalized squared residual $(x - \bar{x})^2/\sigma_x^2$. In our case the residual of what we consider a single astrometric observation x has dimension 2 (having a *right ascension* and a *declination* component). For the sake of the following discussion it is important to notice that in our statistical tests we are not going to use the residuals $x - \bar{x}$ with respect to the average values of the observations $\bar{x}$ (which are of course unknown), but *postfit residuals*

$$\xi = x - \tilde{x}$$

which are differences between the observed values of the astrometric coordinates x (including measurement errors) and the corresponding values $\tilde{x}$ computed by numerical integration starting from the adopted set of orbital elements β. In our case the orbital elements β are not known a priori, but are computed through a least-square fit to the observations x. Therefore they are functions of the stochastic variable x and are to be considered as stochastic variables themselves. If we adopt the convention of using a *tilde* ($\tilde{}$) for indicating quantities which are estimated from (function of) the observations x, we can make this fact explicit by denoting the orbital elements with the symbol $\tilde{\beta}$. As a consequence, the covariance matrix of the residuals Γ_ξ is not equal to the covariance matrix of observation errors Γ_x, but can be computed from it with the approach we describe in the following.

In order to compute the expression of Γ_ξ, we need first to recall the basics of the algorithm of the least-square fit. We will use the following notation:

- N: total number of observations used in the least-square fit;
- t_i: time of observations ($i = 1, 2, \ldots, N$);
- x_i, ξ_i: astrometric observation and residual at a given instant of time t_i (2-dimensional stochastic variables);
- X, Ξ: $2N$-dimensional vectors of all observations and residuals at times $t_1, t_2, \ldots, t_N$

$$X = \begin{pmatrix} x_1 \\ x_2 \\ \vdots \\ x_N \end{pmatrix}; \qquad \Xi = \begin{pmatrix} \xi_1 \\ \xi_2 \\ \vdots \\ \xi_N \end{pmatrix};$$

- $\tilde{\beta}$: solved-for parameters (orbital elements: usually a 6-dimensional stochastic variable);
- A: model matrix ($2N \times 6$) of the least-square fit, equal to the partial derivatives of the value of the observed quantities with respect to the parameters

$$A = \frac{\partial X}{\partial \beta} \begin{pmatrix} \partial \mathcal{F}(t_1)/\partial \beta \\ \partial \mathcal{F}(t_2)/\partial \beta \\ \vdots \\ \partial \mathcal{F}(t_N)/\partial \beta \end{pmatrix}, \tag{1}$$

where $\mathcal{F}(\beta, t)$ is the function mapping the orbital elements β into the astrometric coordinates (right ascension and declination) at time t; in practice, $\mathcal{F}(\beta, t)$ is computed by numerical integration;

γ_i, w_i: 2×2 covariance and weight matrices of single observations x_i (with $w_i = \gamma_i^{-1}$);
Γ, W: $2N \times 2N$ covariance and weight matrices of the observation vector X, with $W = \Gamma^{-1}$.

If we assume, as is the case in the simplified error model, that we are using as a starting point that observations made at different times are uncorrelated ($\mathcal{E}[\xi_i \xi_k] = 0$ if $i \neq k$), these matrices have a simple block-diagonal structure

$$\Gamma = \mathrm{diag}(\gamma_i, \gamma_2, \ldots, \gamma_N);$$
$$W = \mathrm{diag}(w_i, w_2, \ldots, w_N);$$

however, this assumption is not used in the following development, which remains valid in the more general case.

The least-square solution can be computed by integrating numerically the orbit starting from values of the orbital elements β_0 chosen as *reference values*,[1] thus generating a corresponding set of reference (predicted) values of the observations $X_0 = X(\beta_0)$; in a linear approximation, corrections to the orbital elements $\Delta\beta = \beta - \beta_0$ are related to corrections to the observations $\Delta X = X - X_0$ through the relationship

$$\Delta X = A \Delta\beta \tag{2}$$

and the corrections $\Delta\tilde{\beta} = \tilde{\beta} - \beta_0$ satisfying the least-square criterion

$$\Xi' W \Xi = \text{minimum}$$

are given by the expression

$$\Delta\tilde{\beta} = (A'WA)^{-1} A' W \Delta X, \tag{3}$$

where $\Delta X = X - X_0$ are the residuals of the observations with respect to the reference orbit. As is well known, the covariance matrix of the least-square solution $\tilde{\beta}$ is given by

$$\begin{aligned}\Gamma_{\tilde{\beta}} &= \mathcal{E}[\Delta\tilde{\beta}\Delta\tilde{\beta}'] \\ &= (A'WA)^{-1} A' W \mathcal{E}[\Delta X \Delta X'] W A (A'WA)^{-1} \\ &= (A'WA)^{-1} A' W W^{-1} W A (A'WA)^{-1} \\ &= (A'WA)^{-1}\end{aligned} \tag{4}$$

and the residuals Ξ with respect to the least-square orbit are (in the linear approximation)

$$\begin{aligned}\Xi &= X - \widetilde{X} = \Delta X - \Delta\widetilde{X} = \Delta X - A\Delta\tilde{\beta} \\ &= \Delta X - A(A'WA)^{-1} A' W \Delta X \\ &= \left[I - A(A'WA)^{-1} A' W\right] \Delta X,\end{aligned} \tag{5}$$

where I is the unit matrix of dimension $2N \times 2N$. The procedure outlined up to this point is quite classical and ultimately goes back to the work of C.F. Gauss; for more modern accounts of it see for instance Danby (1988, Section 7.5) and Cappellari et al. (1976).

The covariance matrix of the residuals Ξ can be computed directly from their expression of Eq. (5) as

$$\begin{aligned}\Gamma_\Xi = \mathcal{E}[\Xi\Xi'] &= \left[I - A(A'WA)^{-1}A'W\right] \mathcal{E}[\Delta X \Delta X'] \\ &\quad \times \left[I - A(A'WA)^{-1}A'W\right]' \\ &= \left[I - A(A'WA)^{-1}A'W\right] W^{-1} \left[I - WA(A'WA)^{-1}A'\right] \\ &= W^{-1} - A(A'WA)^{-1}A' = \Gamma - A\Gamma_{\tilde{\beta}}A'.\end{aligned}$$

If we indicate with the notation A_i the 2×6 matrix obtained by selecting from matrix A only the two lines related to the observation at time t_i, we can express the covariance matrix of a single residual ξ_i as

$$\gamma_{\xi_i} = \gamma_i - A_i \Gamma_{\tilde{\beta}} A_i'. \tag{6}$$

In a similar way it is possible to compute the covariance matrix of a *prediction residual* ξ^*, namely the residual (with respect to the orbital solution) of an observation (performed, say, at time t^*) which has not been used for the least-square fit; of course, also in this case the linearized relationship between orbital error $\Delta\beta$ and prediction error $\Delta x^*_{\mathrm{pred}}$ has the same form already expressed by Eqs. (1) and (2)

$$\Delta x^*_{\mathrm{pred}} = A^* \Delta\beta, \quad \text{with } A^* = \left(\frac{\partial \mathcal{F}(t^*)}{\partial\beta}\right),$$

and the covariance matrix of the *prediction error* is therefore given by

$$\gamma_{x^*_{\mathrm{pred}}} = \mathcal{E}\left[\Delta x^*_{\mathrm{pred}} \Delta x^{*\prime}_{\mathrm{pred}}\right] = A^* \Gamma_{\tilde{\beta}} A^{*\prime}.$$

In this case, however, the prediction error and the measurement error are uncorrelated, since we have assumed that observations be mutually uncorrelated and the observation x^*_{obs} at time t^* was *not* used in the least-square fit; therefore the covariance matrix of the *prediction error*

$$\xi^* = x^*_{\mathrm{obs}} - x^*_{\mathrm{pred}}$$

is given simply by the sum of the covariances of the two components

$$\begin{aligned}\gamma_{\xi^*} &= \mathcal{E}\left[\left(x^*_{\mathrm{obs}} - x^*_{\mathrm{pred}}\right)\left(x^*_{\mathrm{obs}} - x^*_{\mathrm{pred}}\right)'\right] \\ &= \mathcal{E}\left[x^*_{\mathrm{obs}} x^{*\prime}_{\mathrm{obs}}\right] + \mathcal{E}\left[x^*_{\mathrm{pred}} x^{*\prime}_{\mathrm{pred}}\right] = \gamma^* + \gamma_{x^*_{\mathrm{pred}}} \\ &= \gamma^* + A^* \Gamma_{\tilde{\beta}} A^{*\prime},\end{aligned} \tag{7}$$

where γ^* indicates the covariance matrix of x^*_{obs}. Therefore, if we take into account the possibility that some of the observations are considered as *outliers* and are not used for computing the least-square solution, we must generalize the expression of the covariance of the residual given by Eq. (6) in the following way

$$\gamma_{\xi_i} = \gamma_i \pm A_i \Gamma_{\tilde{\beta}} A_i', \tag{8}$$

where the sign to be used is ± 1 if the observation is an outlier and -1 if the observation is included in the least-square

[1] The reference value β_0 can be selected quite arbitrarily, with the only constraint that it must be close enough to the true solution as to allow the convergence of the subsequent iterative corrections; usually it is the output of a preliminary orbit determination algorithm.

solution. Therefore, the expected error in the residual ξ_i is larger than the observation error in the case of a rejected outlier (the prediction error is an independent source of error which must be added quadratically to the observation error in order to compute the total error), but is smaller if the observation is included in the fit, because the least-square solution has a tendency to interpolate observations (prediction error in the vicinity of an observation tends to go in the same direction as the observation error).

2.4. Outlier rejection: practical application

In practice, outlier rejection is performed in an iterative way in the course of the same iterations which are performed for computing the differential corrections to the orbital elements. Each observation is marked by a *rejection flag* that is used by the program for deciding whether it has to be included in the least-square fit. At each iteration, the program computes the residuals ξ_i of all observations with respect to the corrected orbit, their expected covariance γ_{ξ_i} (according to Eq. (8)) and the corresponding χ^2 value

$$\chi_i^2 = \xi_i \gamma_{\xi_i}^{-1} \xi_i'. \tag{9}$$

If we can assume that the observation errors are distributed normally, then also the distribution of residuals is normal and the value of χ_i^2 has the distribution of a χ^2 variable with 2 degrees of freedom (for instance, 95% of the observations should have $\chi_i^2 < 5.99$ and 99% of the observations should have $\chi_i^2 < 9.21$). Therefore the decision whether to discard (mark as outlier) an observation can be done simply by comparing χ_i^2 with some *threshold value* $\chi_{\rm rej}^2$: the observation is discarded if $\chi_i^2 > \chi_{\rm rej}^2$. (In practice, $\chi_{\rm rej}^2$ is a predefined value chosen somewhat arbitrarily in the range 5–10.) However, although the algorithm is in principle quite simple, its practical implementation presents the following delicate points that deserve particular attention.

1. Since the reference orbit is changed in the course of the iterations and in some cases its initial value can be quite far from the final one, it is necessary to check at each iteration if some of the observations already marked as outliers should be recovered, i.e., returned to the list of observations used for computing the least-square solution. In doing so, some care must be taken in order to avoid the possibility that the rejection process does not terminate, typically because the program enters an infinite loop of rejection and recovery of the same observations in successive iterations. For this reason it is advisable to select the outliers to be recovered according to a criterion of the kind $\chi_i^2 < \chi_{\rm rec}^2$ where $\chi_{\rm rec}^2 < \chi_{\rm rej}^2$ (we are currently using $\chi_{\rm rec}^2 = 7$ and $\chi_{\rm rej}^2 = 8$). We point out that, in principle, if we neglect problems of nonlinearity and rounding-off, such a caution would not be necessary if outlier rejection was accomplished on single observations, applying Eqs. (8) and (9) and performing only one outlier rejection/recovery for each iteration. This is because the value of χ_i^2 supplied by Eq. (9) for an observation included in the fit (using the negative sign in Eq. (8)) is exactly the same which would be obtained by removing that observation from the fit (eliminating the corresponding row in matrix A), computing again the least-square solution (Eq. (3)) and evaluating again Eqs. (8) (using the positive sign) and (9). In practice, however, with data sets containing hundreds or thousands of observation this method would require too much computing time and so we discard/recover several observations at each iteration. Thus the value of χ_i^2 can change and it is necessary to adopt a value of $\chi_{\rm rec}^2 < \chi_{\rm rej}^2$.
2. When the data contain some very distant outliers (observations with very large errors), they affect the solution in such a way that also "good" observations may have quite large residuals and therefore may be rejected on the basis of the χ^2 criterion. As a result a large fraction of the observations could be discarded at the same time, possibly causing problems of convergence. For this reason it is advisable to perform outlier rejection in a "progressive" way, discarding of during the first iterations only the largest outliers and refining the selection only when the orbit is converging toward the final solution. In practice, this is accomplished by finding at each iteration the largest value $\chi_{\rm max}^2$ of the χ_i^2 values for the observations that were included in the fit and discarding only those observations for which the value of χ_i^2 is larger than $\max[\chi_{\rm rej}^2, \alpha\chi_{\rm max}^2]$, where α is chosen in a suitable way in the range $0 < \alpha < 1$ (we are presently using $\alpha = 0.25$). For the same reason of stability it is advisable that the total number of outliers discarded at each iteration does not exceed a certain percentage (5–20%) of the total number of observations available.
3. Since the method of outlier rejection described here is based on statistical estimates, its reliability grows poorer as the number of observations used for the determination of the orbit decreases. If the number of observations is very small a single outlier can affect the solution in such a way that it may become impossible to distinguish the outlier from the correct data points on the basis of orbital residuals alone, and in such cases it is safer to give up completely with automated outlier rejection. From the point of view of the stability of the convergence of the algorithm, it is much better if the transition between the two cases (rejection/no rejection) does not occur abruptly at a certain value of the number of observations N (or, better, of the number of *selected* observations $N_{\rm sel}$, i.e., the number of observations used for the least-square fit), but is as smooth as possible. This can be obtained by adding to the rejection threshold $\chi_{\rm rej}^2$ "fudge term" $\phi(N_{\rm sel})$ which is a smooth function of $N_{\rm sel}$; its expression must be chosen in such a way that $\phi(n)$ is very large for small values of n (say, for $n < 10$) and essentially equal to zero for large n ($n > 50$). For the sake of the present work, we have used

$\phi(n) = 400 \cdot (1.2)^{-n}$.

4. As we discuss in detail in Section 4, the use of a statistical model that describes correctly the dispersion (RMS error) of observations but neglects their correlations has the effect of *overweighting* the contribution of observations that are grouped in a short interval of time. On average, this means overweighting modern CCD observations (especially those produced by large surveys) at the expense of older measurements, which are usually much less dense in time. In some cases this can produce an abnormal increase in the residuals for observations that are more sparse in time, which may therefore be rejected; this usually has the effect of weakening the orbital solution, especially if it results in a shortening of the total time span of observations. This problem can be solved completely only by estimating the correlations between observations and introducing these estimates in the stochastic model of the least-square fit. Lacking such a rigorous solution, it can be advisable to limit in some way the rejection of sparse or isolated observations and in particular to avoid discarding all the measurements belonging to one opposition of the asteroid. In this first iteration of the procedure, however, we have not introduced any limitation of this kind in the algorithm for outlier rejection.

For the sake of clarity, we note that the form of the χ^2 test expressed by Eqs. (8) and (9) is the same whether we take into account in the statistical model the correlations between different observations. This is due to the very nature of the decision process, which must assess *separately* and *independently* for each observation whether it has to be discarded or not. In statistical terms this means to compare the residual of the observation with its expected variance, namely with the 2×2 block of the total covariance matrix pertaining to that observation. Therefore correlations among different observations are not relevant: they affect the result of the test only indirectly, by determining the value of the covariance matrix of the orbital parameters $\Gamma_{\tilde{\beta}}$ through Eq. (4).

2.5. Outlier rejection: results

To assess the performance of the automated outlier rejection scheme we present in Fig. 1 the distribution of the postfit RMS of normalized residuals for the objects in our sample. We have excluded from this histogram the cases in which there are radar astrometric observations, because the relative weighting of the radar and optical observations is a problem which needs to be solved, as discussed in Section 5. The RMS displayed in Fig. 1 does not include the residuals for rejected outliers. The relative number of rejections is documented in Fig. 2. The small tail of asteroids for which the rejections are a comparatively large fraction of the observations (for 2% of the cases, the rejections are $> 20\%$) is essentially due to the processing of very old observations, including the ones from the 19th century, together with the more accurate modern ones.

Another way to measure the effectiveness of the automatic outlier removal is to determine how well the residuals

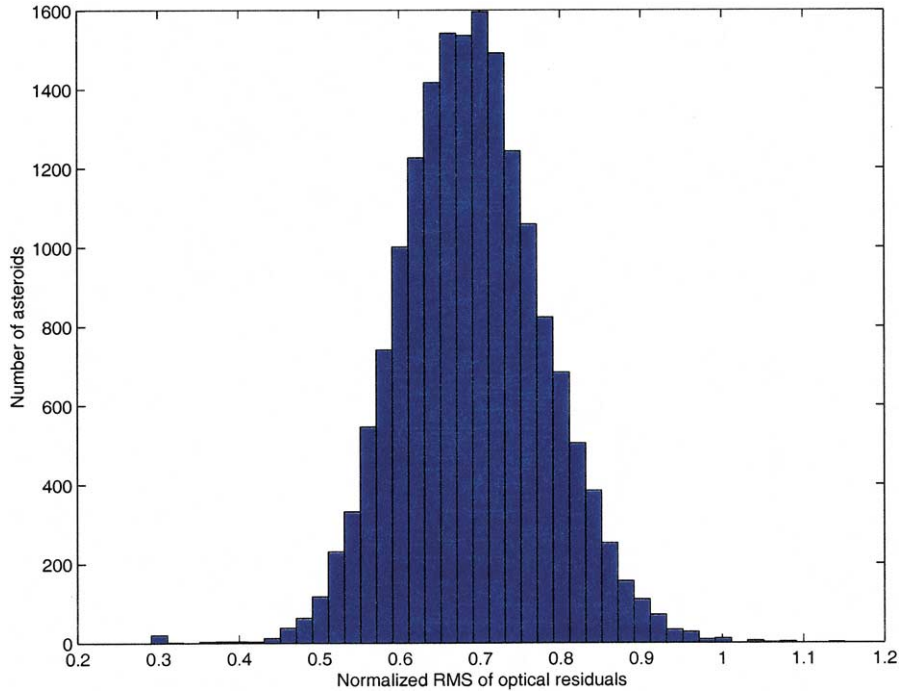

Fig. 1. Histogram of the postfit RMS of the normalized residuals of all optical observations of all the 17,349 asteroids numbered (up to 19 September 2000). The residuals are normalized by the weights used in the least-square orbit estimation, specifically, observations before 1890 use 3 arcsec, those before 1950 use 2 arcsec, and for observations after 1950 the weight corresponds to 1 arcsec. Thus the figure can be interpreted as scaled in arcsec for modern observations, which comprise the vast majority of the data set.

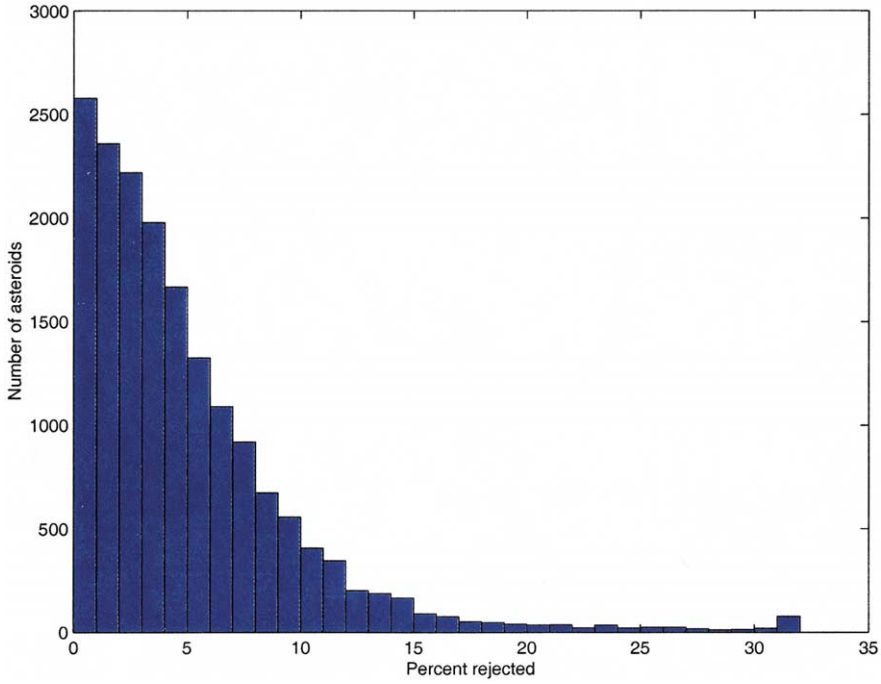

Fig. 2. Histogram of the percentage of rejected outliers among the catalog of 17,349 numbered asteroids.

that have not been rejected fit a Gaussian distribution. This is related to the issue of whether the errors are normally distributed, in that this assumption can apply only after the outliers have been removed. In other words, the errors are in fact not Gaussian, and we are removing the outliers with the goal of using in the fit only those observations for which the errors are Gaussian. This argument is not necessarily as circular as it first appears because it is based on the assumption that the distribution of residuals comprises two separate distributions: a *core* distribution which is Gaussian and is produced by the routine performance of the observing system and an anomalous (outlier) distribution, generated by the sporadic occurrence of different mechanisms. This second distribution is hopefully much less populated but has a much larger RMS; of course, the sum of the two distributions is not normal even if the two components are in themselves normal. The algorithm of outlier rejection is designed in such a way as to eliminate the significant elements of the second contribution while keeping almost unmodified the core distribution (apart from trimming its extreme wings); therefore, the assumption of normality of the core distribution can be checked by a statistical analysis of the residuals.

As the best test of the distribution of residuals, we have used the data set taken from a single observatory, namely LINEAR (observatory code 704), the survey with more observations than any other, thanks to a fully automated system based on a very sensitive CCD. Figure 3 shows both the total data set, in which a non-Gaussian tail is evident, and the set of nonrejected residuals, which approximate the Gaussian shape. Apparently, the automated outlier rejection algorithm is very effective in eliminating the non-Gaussian tail of large residuals. Unavoidably it even removes a little more than needed to follow a Gaussian distribution, but the relative number of such overzealous rejections is very small. These few borderline cases generally will not significantly impact the orbital solution, and anyway this has a negligible effect on the global statistics.

3. Standard deviation statistics

3.1. Data binning

Astrometric observations have to be subdivided by observatory, and within each observatory piece of by means of every piece of information we have on the possible changes in the levels of accuracy. In the observations available from the MPC as a global, homogeneous data set we have only three sources of information, apart from the observatory code. A code in the MPC public observation format indicates the technology used for the observations, e.g., P for photographic measurements, C for CCD camera. The number of digits reported for the time and for the measured angles is an indication of the precision, although it is not clear whether this is the result of an assessment done at the observatory or at the MPC.[2] Finally the time at which the observation was

[2] In order to avoid misunderstandings we have to specify that we use the number of digits of the observed quantities only for the sake of dividing the measurements of a given site into homogeneous batches and not as a quantitative estimate of their accuracy (which is derived from the statistical analysis described below). In other words if a given observatory publishes some of its measurements to, say, 0.1 arcsec in declination, and some other to 0.01 arcsec, we simply perform separate statistics on the two sets, without making any assumption on its results.

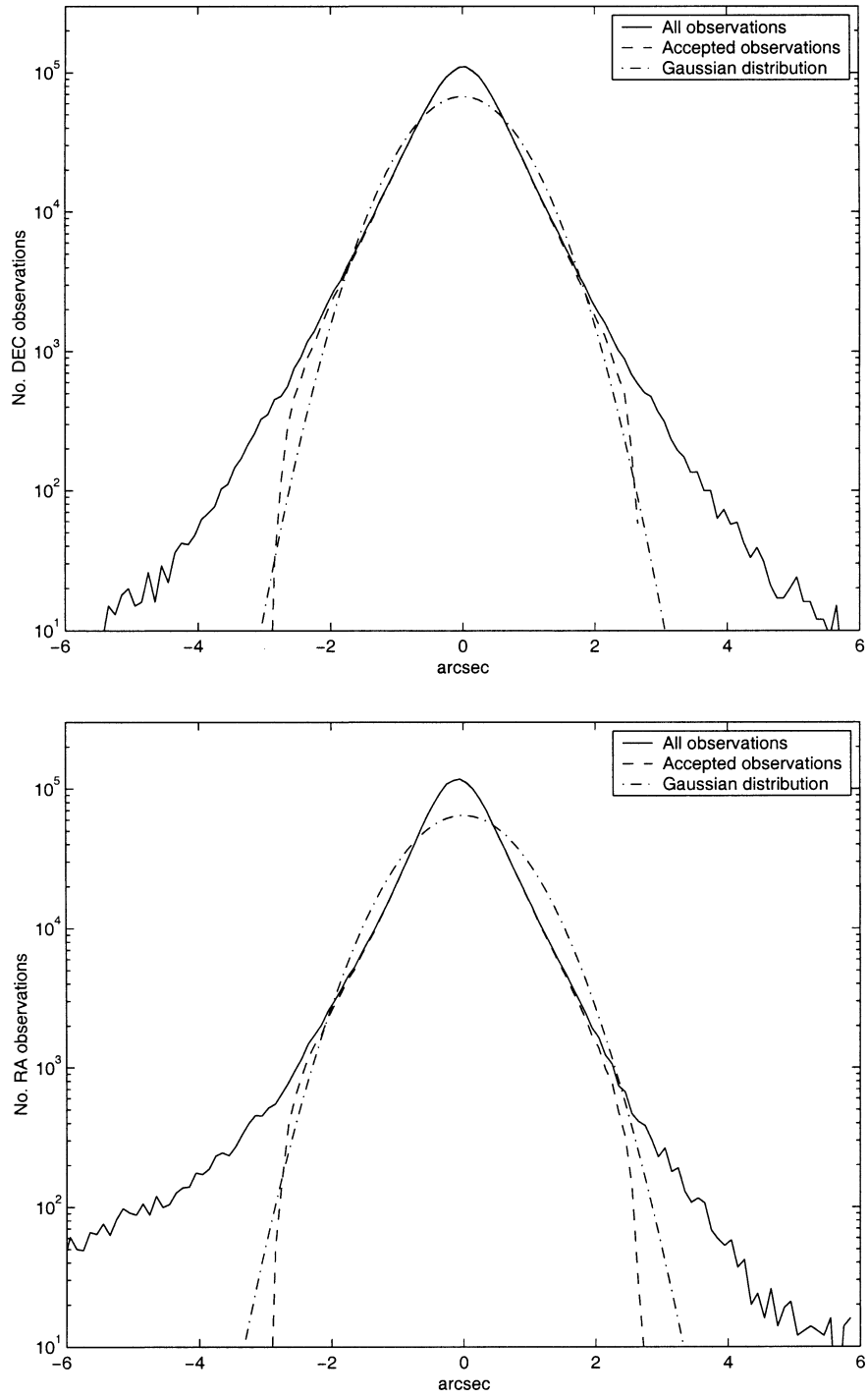

Fig. 3. Histogram of the residuals of all observations by the LINEAR survey, in declination (above) and right ascension (below). The dashed lines refer to the observations accepted by the automatic rejection algorithm described in Section 2.

taken is certainly relevant, since the observatories improve their technology and the reduction procedures over time, and often the skills of the observers also improve with experience.

Thus for each observatory, each technology code, and each number of reported digits, we form time bins such that there are enough data in each one; we currently require at least 50 observations per bin. The binning algorithm begins with equal time intervals of 400 days; consecutive bins are joined if they contain < 50 observations, with a maximum length of 4000 days. If an observatory has too few observations of a given class the binning procedure may fail and the data cannot be analyzed in this way to avoid the problems of small number statistics. However, even these data are used by bundling together the residuals from all observatories with few data.

3.2. Estimation of the RMS and bias

For each batch of data we have computed the RMS of the residuals separately for declination δ and for right ascension α; residuals in α need to be multiplied by $\cos\delta$ because of the metric of the unit sphere. This, however, is only the first step of a procedure which must account for the fact that there are spurious and grossly wrong observations (outliers). These large residuals have to be removed to avoid contamination of the computed statistics. The underlying assumption is again that the distribution of the residuals is in fact not Gaussian, but can become Gaussian through outlier removal. To avoid a circular argument, we need to show that the removal of some outliers is appropriate because it is an empirically verified fact that the distribution of the residuals is not Gaussian. This is achieved in a very immediate way by plotting histograms of residuals (separately for each bin), as already shown in Fig. 3, which clearly shows a tail of comparatively large residuals by far exceeding what would occur for a Gaussian.

A quantitative way to measure the deviation of a set of residuals ξ_i from a Gaussian distribution is to compute the *kurtosis*

$$k(\xi) = \frac{n\sum_{i=1}^{n}\xi_i^4}{\left[\sum_{i=1}^{n}\xi_i^2\right]^2}$$

which should be 3 if the distribution were Gaussian. The kurtosis, because of the presence of the fourth power of the residuals, is strongly sensitive to the presence of outliers; for instance, introducing a single 10-σ outlier in a normal distribution of 100 data points has the effect of increasing the value of the kurtosis from 3 to about 26. The kurtosis for the full set of residuals shown in Fig. 3 is 7006 for right ascension and 213 for declination. This shows that some outlier rejection scheme needs to be used.

The procedure to remove the outliers from the statistical analysis is an iterative one, which attempts to converge to a partition of the residuals of a given bin into a subset of "outliers" and a subset, representing a Gaussian distribution. At each iteration, the RMS and kurtosis are computed for the non-outliers, and the list of outliers is increased by adding the largest residuals if the kurtosis is > 3. At the end, the kurtosis of the non-outliers is just below 3, that is, it would become > 3 by discarding one outlier less. When the number of observations in the bin is large the non-outliers represent a good approximation to a Gaussian and the distribution of their residuals is well described by only two parameters, the RMS and the mean, or bias. Note that this procedure is different, and independent of, the outlier rejection scheme used in the orbit determination (described in Section 2), where we were assuming we already know the variance of the core distribution, which is what we wish to estimate here. That is, some residuals which have not been used in the orbital solution can be considered in the error statistics, and also the converse; this is advisable also because it keeps as separate as possible the stages of orbit determination and statistical analysis.

Tables 1 and 2 list the RMS and bias, as well as others parameters useful to assess the station performance, for the 77 bins containing more than 3000 observations. These bins comprise 67% of the data, even though they are only 2% of the bins. The data for all observatories and all bins are available upon request and are distributed with the OrbFit software.

The results of our RMS estimation for the largest bins, the same listed in Tables 1 and 2, are summarized in Fig. 4. There is a clear trend toward lower RMS for the more recent observations, at least for the observatories currently contributing the most data. However, for a given time there is a very significant scatter of RMS values; while a difference by a factor < 2 might not make a big difference in the least-square solutions, a difference by a factor 10 can affect the results in a very significant way.

The results for the bias are summarized in Fig. 5, which shows the number of observations with given ratio between bias and RMS. The histograms are based only on the largest bins, again those listed in Tables 1 and 2. The figure clearly shows that the bias should be taken into account in a realistic model of the observation errors. There are several isolated peaks, especially in declination, which are associated with some of the bins containing more data. For example, the most recent declination observations from LINEAR have a bias $0.39 \times$ RMS, the ones from LONEOS have a bias $0.83 \times$ RMS, and these two batches largely contribute to the two peaks on the right of the histogram. These biased batches are so large that the rest of the data are biased toward negative residuals to preserve the zero mean of all the residuals which is enforced by the least-square solutions. That is, the orbits have been shifted somewhat north with respect to the solutions which would be obtained if the observational bias were corrected for in the orbit determination process.

The interpretation of the biases is not easy. The presence of a comparatively large bias in declination for many observatories using Schmidt telescopes could point to the problems arising from deformations in the star images. But similar problems appear in telescopes with different optical systems, such as LINEAR. Even more puzzling is the fact that the bias appears to change with time, and in some cases, including the two examples cited above, appears larger in the most recent data. Our intent is only to provide this information to all the major observatories for them to analyze and discuss the possible causes and the corrective actions which may be possible.

3.3. Limitations and possible improvements

The procedure outlined in the previous section has three main limitations in describing the error statistics. First, it does not reflect all the systematic errors, it just bundles them together with random errors to compute a realistic RMS and bias.

Table 1
Observation error statistics—declination

Prec. (″)	Obs. type	Date range	N_{obs}	k_{all}	Rej. (%)	RMS (″)	Bias (″)	Bias / RMS
046—Klet Observatory, Ceske Budejovice								
0.1	C	1995-10-10–1996-11-13	3340	5.7	3.14	0.39	0.00	0.00
0.1	C	1996-11-13–1997-12-18	3130	5.3	3.99	0.34	0.05	0.14
095—Crimea-Nauchnij								
0.1	A	1978-04-02–1979-05-07	3489	1991.0	3.21	1.24	0.34	0.27
0.1	A	1979-05-07–1980-06-10	3020	1835.0	3.61	1.59	−0.25	−0.16
0.1	A	1982-08-19–1983-09-23	4417	183.3	3.98	1.50	0.18	0.12
0.1	A	1990-04-19–1995-10-10	3364	262.0	1.90	2.13	−0.26	−0.12
106—Crni Vrh								
0.1	C	1999-01-22–2000-02-26	4136	1377.0	5.61	0.39	0.16	0.41
120—Visnjan								
0.1	C	1997-12-18–1999-01-22	3725	112.5	3.65	0.44	0.02	0.05
0.1	C	1999-01-22–2000-02-26	5988	7.9	2.84	0.47	−0.07	−0.15
327—Peking Observatory, Xinglong Station								
0.1	C	1995-10-10–1996-11-13	4524	7.0	1.88	0.45	0.04	0.09
0.1	C	1996-11-13–1997-12-18	6554	16.4	2.85	0.39	0.10	0.27
0.1	C	1997-12-18–1999-01-22	6254	8.2	3.47	0.37	0.10	0.26
413—Siding Spring Observatory								
10.1	A	1980-06-10–1981-07-15	7630	120.4	1.91	0.95	−0.18	−0.19
566—Haleakala-NEAT/GEODSS								
0.1	C	1993-08-01–1996-11-13	7927	10.9	4.60	0.57	−0.07	−0.13
0.1	C	1996-11-13–1997-12-18	6345	61.6	3.69	0.51	0.16	0.31
0.1	C	1997-12-18–1999-01-22	17454	5.1	2.34	0.62	−0.18	−0.29
608—Haleakala-AMOS								
0.1	C	2000-02-26–2000-09-19	11329	6.8	4.36	0.59	−0.39	−0.66
675—Palomar Mountain								
0.1	A	1959-08-20–1962-12-02	4754	38.2	1.07	0.69	−0.06	−0.08
0.1	A	1970-08-02–1972-10-10	3343	1504.0	0.84	1.16	−0.77	−0.66
0.1	A	1972-10-10–1974-12-19	5813	100.2	0.71	1.34	−0.66	−0.49
0.1	A	1977-02-26–1978-04-02	4192	696.9	0.95	1.15	−0.44	−0.38
0.1	A	1989-03-15–1990-04-19	3359	302.3	3.57	1.13	−0.90	−0.79
0.1	A	1990-04-19–1991-05-24	8991	68.8	2.15	1.03	−0.71	−0.69
0.1	A	1991-05-24–1992-06-27	6002	972.0	3.15	0.93	−0.64	−0.69
0.1	P	1988-02-09–1989-03-15	4849	3.8	0.56	0.96	−0.24	−0.25
0.1	P	1989-03-15–1990-04-19	3495	7.3	1.00	0.85	−0.03	−0.03
0.1	P	1990-04-19–1991-05-24	5227	6.1	0.48	0.90	−0.03	−0.03
0.1	P	1991-05-24–1992-06-27	6818	122.3	1.45	0.87	−0.35	−0.40
0.1	P	1992-06-27–1993-08-01	6075	1077.0	0.94	0.86	−0.11	−0.12
0.1	P	1993-08-01–1994-09-05	8324	122.4	0.61	0.89	−0.24	−0.27
0.1	P	1994-09-05–1995-10-10	3213	3.5	0.53	0.89	−0.18	−0.20
688—Lowell Observatory, Anderson Mesa Station								
0.1	A	1980-06-10–1981-07-15	3380	81.5	2.78	1.06	−1.65	−1.55
0.1	A	1981-07-15–1982-08-19	4330	319.0	1.45	1.33	−1.97	−1.48
0.1	A	1982-08-19–1983-09-23	5159	64.9	2.56	1.06	−1.43	−1.35
0.1	A	1983-09-23–1984-10-27	4647	17.1	1.66	1.13	−1.49	−1.31
0.1	A	1984-10-27–1985-12-01	3586	82.9	2.04	1.18	−0.47	−0.40
689—US Naval Observatory, Flagstaff								
0.1	C	1997-12-18–1999-01-22	26516	11.9	6.29	0.13	−0.00	−0.01
0.1	c	1999-01-22–2000-09-19	29511	11.2	7.01	0.14	−0.03	−0.22
691—Steward Observatory, Kitt Peak-Spacewatch								
0.1	c	1990-04-19–1992-06-27	3891	16.9	2.18	0.40	0.06	0.14
0.1	c	1993-08-01–1994-09-05	3260	12.8	3.50	0.31	0.04	0.12
0.1	c	1994-09-05–1995-10-10	5105	14.7	3.37	0.30	−0.05	−0.15
0.1	c	1995-10-10–1996-11-13	5884	18.2	2.19	0.28	−0.03	−0.12
0.1	c	1996-11-13–1997-12-18	5666	23.5	2.49	0.32	−0.02	−0.07
0.1	c	1997-12-18–1999-01-22	7993	12.8	3.32	0.29	−0.01	−0.04
0.1	C	1999-01-22–2000-02-26	13013	27.1	4.15	0.29	−0.09	−0.31
0.1	C	2000-02-26–2000-09-19	6157	10.3	3.54	0.30	−0.18	−0.61
699—Lowell Observatory-LONEOS								
0.1	C	1996-11-13–1999-01-22	42995	20.8	1.99	0.52	0.19	0.37
0.1	C	1999-01-22–2000-02-26	56339	12.5	2.54	0.47	0.39	0.83

Table 1 (*continued*)

Prec. (″)	Obs. type	Date range	N_{obs}	k_{all}	Rej. (%)	RMS (″)	Bias (″)	Bias RMS
0.1	C	2000-02-26–2000-09-19	26756	5.1	4.06	0.39	0.16	0.40
0.1	c	1999-01-22–2000-09-19	26180	8.7	3.42	0.33	0.16	0.49
703—Catalina Sky Survey								
0.1	c	1999-01-22–2000-02-26	43723	14.9	7.44	0.34	0.28	0.82
0.1	c	2000-02-26–2000-09-19	7148	40.2	5.19	0.36	0.21	0.58
7041—Lincoln Laboratory ETS, New Mexico								
0.1	C	1996-11-13–1997-12-18	16328	7.0	3.82	0.75	0.11	0.15
0.1	c	1997-12-18–1999-01-22	184448	5.6	2.65	0.80	0.02	0.03
0.1	c	1999-01-22–2000-02-26	376635	552.8	3.35	0.60	−0.02	−0.03
0.1	c	2000-02-26–2000-09-19	236411	46.5	3.76	0.49	0.19	0.39
801—Oak Ridge Observatory								
0.1	A	1990-04-19–1991-05-24	3193	26.0	3.51	0.44	−0.01	−0.03
0.1	C	1992-06-27–1993-08-01	4035	9.8	3.62	0.45	−0.07	−0.15
0.1	C	1993-08-01–1994-09-05	3608	5.8	3.77	0.48	−0.01	−0.03
0.1	C	1994-09-05–1995-10-10	3479	5.4	4.25	0.49	−0.03	−0.06
0.1	C	1995-10-10–1996-11-13	3438	4.2	2.76	0.55	−0.29	−0.52
809—European Southern Observatory, La Silla								
0.1	A	1981-07-15–1982-08-19	3638	821.3	3.79	0.69	0.02	0.02
0.1	A	1983-09-23–1984-10-27	4672	9.4	1.90	0.58	−0.04	−0.07
0.1	A	1984-10-27–1985-12-01	4973	1635.0	1.77	0.63	−0.03	−0.05
0.1	A	1985-12-01–1987-01-05	5572	506.5	3.43	0.54	0.01	0.02
0.1	A	1987-01-05–1988-02-09	7351	1558.0	4.65	0.64	−0.09	−0.14
0.1	A	1988-02-09–1989-03-15	6203	26.1	7.54	0.69	−0.08	−0.11
0.1	A	1989-03-15–1990-04-19	6400	1349.0	4.69	0.94	−0.27	−0.29
0.1	A	1990-04-19–1991-05-24	9304	1500.0	2.57	0.99	−0.15	−0.15
0.1	A	1991-05-24–1992-06-27	4663	450.3	2.55	1.03	−0.03	−0.03
0.1	P	1991-05-24–1992-06-27	3918	7.6	1.30	1.22	−0.13	−0.11
0.1	P	1992-06-27–1993-08-01	5721	4.2	3.37	1.24	−0.14	−0.11
0.1	P	1993-08-01–1994-09-05	8850	5.5	0.58	1.72	0.43	0.25
0.1	P	1995-10-10–1996-11-13	5806	10.4	0.22	1.77	0.63	0.35
0.1	P	1996-11-13–1997-12-18	4741	3.7	0.84	1.72	0.52	0.30
0.1	P	1997-12-18–2000-09-19	6179	3.0	0.00	1.96	0.67	0.34
910—Caussols-ODAS								
0.1	C	1997-12-18–1999-01-22	5531	4.2	0.43	0.52	−0.02	−0.05

Note. The following definitions describe the table entries: "Prec." is the reported precision of the observations, "Obs. type" is the observation method code reported by the MPC, "Date range" indicates the duration of the time bin considered, N_{obs} is the number of observations, k_{all} is the kurtosis of all observations before outlier rejection, "Rej." is the percentage of observations rejected to obtain kurtosis ~ 3, "RMS" is the root mean square relative to the mean, and "Bias" is the mean of the residuals in each bin.

Second, the bundling of residuals into bins should allow us to process homogeneous data, but this is not always the case, because we do not have enough information. The same observatory code could correspond to different telescopes at the same site: e.g., the code 675 corresponds to various telescopes on Mount Palomar (with apertures ranging from 60 to 500 cm). The information on the telescope used in each observation run is not available in a format usable for large scale processing. The same applies to the information on the reduction procedure, including the star catalog used. The information on the individual observation, such as the exposure time and the sky background level, is not available at all; thus the signal to noise ratio of the individual observation, which could vary by orders of magnitude even for the same telescope and the same apparent magnitude of the target, cannot be computed. The MPC has recently proposed an expanded observation format (ftp://cfa-ftp.harvard.edu/pub/MPC/) which would substantially improve this situation in the long run.

Another source of non-uniformity among the data of a given bin could arise from the arbitrary time boundaries we have used for our bins. If an observatory has substantially upgraded its equipment or procedures at a date in the middle of one of these bins, the binning should be revised to incorporate this information.

Third, there is some information which in principle could be used to form more homogeneous bins of residuals, but which we have not used in the present work. The two main parameters which are certainly relevant are the proper motion and the apparent magnitude.

Inaccuracy of the measurements due to trailing and to timing errors is a function of the proper motion. If this effect is important, the RMS computed on bins of data dominated by observations of main belt asteroids could be an underestimation of the error for near Earth asteroids (NEAs). Unfortunately the trailing error is a function also of the exposure time, which is not available, and for the timing error very little a priori information is available, although it is easy

Table 2
Observation error statistics—right ascension

Prec. (″)	Obs. type	Date range	N_{obs}	k_{all}	Rej. (%)	RMS (″)	Bias (″)	Bias / RMS
046—Klet Observatory, Ceske Budejovice								
0.01	C	1995-10-10–1996-11-13	3340	9.7	5.21	0.37	−0.01	−0.01
0.01	C	1996-11-13–1997-12-18	3130	5.2	2.17	0.39	−0.04	−0.11
095—Crimea-Nauchnij								
0.01	A	1978-04-02–1979-05-07	3489	17.6	2.26	1.40	−0.67	−0.48
0.01	A	1979-05-07–1980-06-10	3020	2699.0	1.46	1.89	−0.21	−0.11
0.01	A	1982-08-19–1983-09-23	4416	805.3	1.65	1.83	−0.07	−0.04
0.01	A	1990-04-19–1995-10-10	3364	274.9	3.27	1.77	−0.31	−0.18
106—Crni Vrh								
0.01	C	1999-01-22–2000-02-26	4133	8.6	6.00	0.40	−0.04	−0.10
120—Visnjan								
0.01	C	1997-12-18–1999-01-22	3725	23.4	7.65	0.55	0.03	0.05
0.01	C	1999-01-22–2000-02-26	5988	7.7	3.77	0.62	−0.07	−0.11
327—Peking Observatory, Xinglong Station								
0.01	C	1995-10-10–1996-11-13	4524	36.3	2.70	0.44	0.03	0.08
0.01	C	1996-11-13–1997-12-18	6554	327.1	2.21	0.47	−0.02	−0.03
0.01	C	1997-12-18–1999-01-22	6254	13.9	6.86	0.34	−0.03	−0.08
413—Siding Spring Observatory								
0.01	A	1980-06-10–1981-07-15	7630	6.8	2.79	1.28	−0.09	−0.07
566—Haleakala-NEAT/GEODSS								
0.01	C	1994-09-05–1996-11-13	7915	23.7	4.94	0.47	−0.07	−0.14
0.01	C	1996-11-13–1997-12-18	6345	35.5	5.23	0.44	−0.12	−0.27
0.01	C	1997-12-18–1999-01-22	17454	7.2	3.57	0.49	−0.03	−0.07
608—Haleakala-AMOS								
0.01	C	2000-02-26–2000-09-19	11329	52.4	2.40	0.59	−0.09	−0.15
675—Palomar Mountain								
0.01	A	1959-08-20–1962-12-02	4754	27.6	2.15	0.59	0.03	0.05
0.01	A	1970-08-02–1972-10-10	3343	10.1	4.34	1.08	−0.17	−0.16
0.01	A	1972-10-10–1974-12-19	5813	243.6	2.49	1.10	0.24	0.22
0.01	A	1977-02-26–1978-04-02	4186	34.3	2.60	1.03	0.13	0.13
0.01	A	1989-03-15–1990-04-19	3359	507.0	4.82	0.96	−0.10	−0.10
0.01	A	1990-04-19–1991-05-24	8991	134.1	4.72	0.77	0.04	0.05
0.01	A	1991-05-24–1992-06-27	6002	240.5	2.87	0.79	0.06	0.07
0.01	P	1988-02-09–1989-03-15	4849	14.7	3.05	0.71	0.05	0.07
0.01	P	1989-03-15–1990-04-19	3495	11.1	2.58	0.71	0.04	0.06
0.01	P	1990-04-19–1991-05-24	5227	6.1	2.41	0.73	−0.16	−0.22
0.01	P	1991-05-24–1992-06-27	6818	48.4	3.30	0.65	−0.00	−0.00
0.01	P	1992-06-27–1993-08-01	6075	383.0	3.31	0.66	−0.01	−0.02
0.01	P	1993-08-01–1994-09-05	8324	7.5	3.87	0.66	−0.06	−0.09
0.01	P	1994-09-05–1995-10-10	3213	8.3	2.86	0.64	0.00	0.00
688—Lowell Observatory, Anderson Mesa Station								
0.01	A	1980-06-10–1981-07-15	3380	197.2	4.08	0.95	0.59	0.62
0.01	A	1981-07-15–1982-08-19	4330	312.7	4.32	1.12	0.72	0.64
0.01	A	1982-08-19–1983-09-23	5159	18.9	4.69	0.96	0.45	0.47
0.01	A	1983-09-23–1984-10-27	4647	9.9	5.34	1.05	0.62	0.59
0.01	A	1984-10-27–1985-12-01	3586	18.0	4.04	1.09	0.51	0.47
689—US Naval Observatory, Flagstaff								
0.001	C	1997-12-18–1999-01-22	26516	11.4	4.25	0.13	−0.01	−0.05
0.001	C	1999-01-22–2000-09-19	29511	12.5	4.37	0.13	−0.01	−0.11
691—Steward Observatory, Kitt Peak-Spacewatch								
0.01	C	1999-01-22–2000-02-26	13013	12.6	3.15	0.36	−0.04	−0.12
0.01	C	2000-02-26–2000-09-19	6157	5.8	1.90	0.38	−0.23	−0.61
0.01	c	1990-04-19–1992-06-27	3891	8.8	3.14	0.49	−0.08	−0.15
0.01	c	1993-08-01–1994-09-05	3260	8.2	4.05	0.40	−0.13	−0.33
0.01	c	1994-09-05–1995-10-10	5105	16.1	4.72	0.33	−0.10	−0.32
0.01	c	1995-10-10–1996-11-13	5890	979.7	2.89	0.38	−0.09	−0.25
0.01	c	1996-11-13–1997-12-18	5666	6.3	1.15	0.40	−0.11	−0.28
0.01	c	1997-12-18–1999-01-22	7993	5.2	0.49	0.53	−0.14	−0.27
699—Lowell Observatory-LONEOS								
0.01	C	1996-11-13–1999-01-22	42995	1536.0	2.41	0.51	0.03	0.06
0.01	C	1999-01-22–2000-02-26	56339	594.2	1.35	0.54	0.06	0.11

Table 2 (*continued*)

Prec. (″)	Obs. type	Date range	N_{obs}	k_{all}	Rej. (%)	RMS (″)	Bias (″)	Bias RMS
0.01	C	2000-02-26–2000-09-19	26756	4.7	2.91	0.49	−0.02	−0.05
0.01	c	1999-01-22–2000-09-19	26180	4.8	2.44	0.40	0.05	0.11
703—Catalina Sky Survey								
0.01	c	1999-01-22–2000-02-26	43723	10.4	6.55	0.39	−0.04	−0.10
0.01	c	2000-02-26–2000-09-19	7148	10.6	6.21	0.38	0.03	0.08
704—Lincoln Laboratory ETS, New Mexico								
0.01	C	1996-11-13–1997-12-18	16328	6.6	5.36	0.95	0.17	0.18
0.01	C	1997-12-18–1999-01-22	184448	7.0	3.92	0.79	−0.03	−0.03
0.01	C	1999-01-22–2000-02-26	376635	16220.0	4.22	0.56	0.02	0.04
0.01	C	2000-02-26–2000-09-19	236411	10.5	5.05	0.45	0.06	0.14
801—Oak Ridge Observatory								
0.01	A	1990-04-19–1991-05-24	3193	11.0	3.88	0.37	−0.02	−0.06
0.01	C	1992-06-27–1993-08-01	4035	9.1	3.57	0.40	−0.03	−0.07
0.01	C	1993-08-01–1994-09-05	3608	10.1	5.13	0.43	−0.01	−0.03
0.01	C	1994-09-05–1995-10-10	3479	6.0	3.68	0.49	−0.02	−0.04
0.01	C	1995-10-10–1996-11-13	3438	5.8	5.76	0.37	0.05	0.14
809—European Southern Observatory, La Silla								
0.01	A	1981-07-15–1982-08-19	3638	187.8	5.31	0.77	−0.12	−0.16
0.01	A	1983-09-23–1984-10-27	4672	20.6	2.72	0.68	−0.16	−0.23
0.01	A	1984-10-27–1985-12-01	4973	1622.0	2.65	0.73	−0.14	−0.19
0.01	A	1985-12-01–1987-01-05	5572	74.6	3.66	0.66	−0.12	−0.18
0.01	A	1987-01-05–1988-02-09	7351	2203.0	4.72	0.73	−0.01	−0.01
0.01	A	1988-02-09–1989-03-15	6203	115.8	6.50	0.80	−0.03	−0.04
0.01	A	1989-03-15–1990-04-19	6400	2193.0	5.00	0.96	−0.02	−0.02
0.01	A	1990-04-19–1991-05-24	9304	18.6	3.45	1.01	−0.03	−0.03
0.01	A	1991-05-24–1992-06-27	4663	756.0	2.90	1.12	0.11	0.10
0.01	P	1991-05-24–1992-06-27	3918	12.8	3.39	1.14	−0.18	−0.16
0.01	P	1992-06-27–1993-08-01	5721	7.1	4.46	1.16	0.13	0.11
0.01	P	1993-08-01–1994-09-05	8850	328.5	1.90	1.44	0.51	0.36
0.01	P	1995-10-10–1996-11-13	5806	125.5	0.95	1.50	0.55	0.37
0.01	P	1996-11-13–1997-12-18	4741	5.9	3.25	1.34	0.33	0.24
0.01	P	1997-12-18–2000-09-19	6179	4.6	0.44	1.64	0.85	0.52
910—Caussols-ODAS								
0.01	C	1997-12-18–1999-01-22	5531	2.9	0.00	1.06	−0.09	−0.08

Note. See Table 1 for column definitions.

to identify a posteriori. These two errors can be detected when large residuals have a significant correlation between right ascension and declination. Measurement errors due to both trailing and time errors could be relevant in degrading some observations of NEAs. The most dramatic example of this kind is the large data set of observations of (1566) Icarus during its close approach at 0.04 AU from Earth in 1968. In our present solution more than 100 observations are discarded because of timing errors, but in this way the information on the position across track, which could be accurate, is also lost. Other infamous cases are 1937 UB and 1954 XA, both discovered during close approaches to the Earth and lost after few days, with orbits made even more unreliable by timing uncertainties. In the future we plan to be able to handle timing–trailing errors by introducing right ascension–declination correlation in the least-square fit algorithm.

There is no doubt that an observation with a low signal to noise ratio will have larger errors. Although the relative signal strength is typically a function of apparent magnitude, it is, unfortunately, not a function of magnitude only. It also depends strongly upon exposure time, pixel size, and seeing conditions, none of which is available to us. For this reason we have not used binning based upon the apparent magnitude, but we may explore the value of this in the future.

4. Correlation analysis

Even after the residuals have been rescaled with the appropriate weights, and shifted by appropriate biases, it is not the case that their probability distributions are correctly represented by independent, unit variance Gaussian functions. In intuitive terms, the error in each observation has a higher probability of having the same sign, even a similar value, as the previous one. For Gaussian distributions, independence and zero correlation are equivalent; thus we can test the hypothesis of independence by measuring the correlation of a set of couples of residuals (ξ_i, ξ_j), with $(i, j) \in B$:

$$\mathrm{Corr}(\xi, B) = \frac{1}{N_B} \sum_{(i,j)\in B} \xi_i \sqrt{w_i} \xi_j \sqrt{w_j}, \tag{10}$$

where w_i is the weight associated with the residual ξ_i, that is the inverse of the variance of the residual in its supposedly

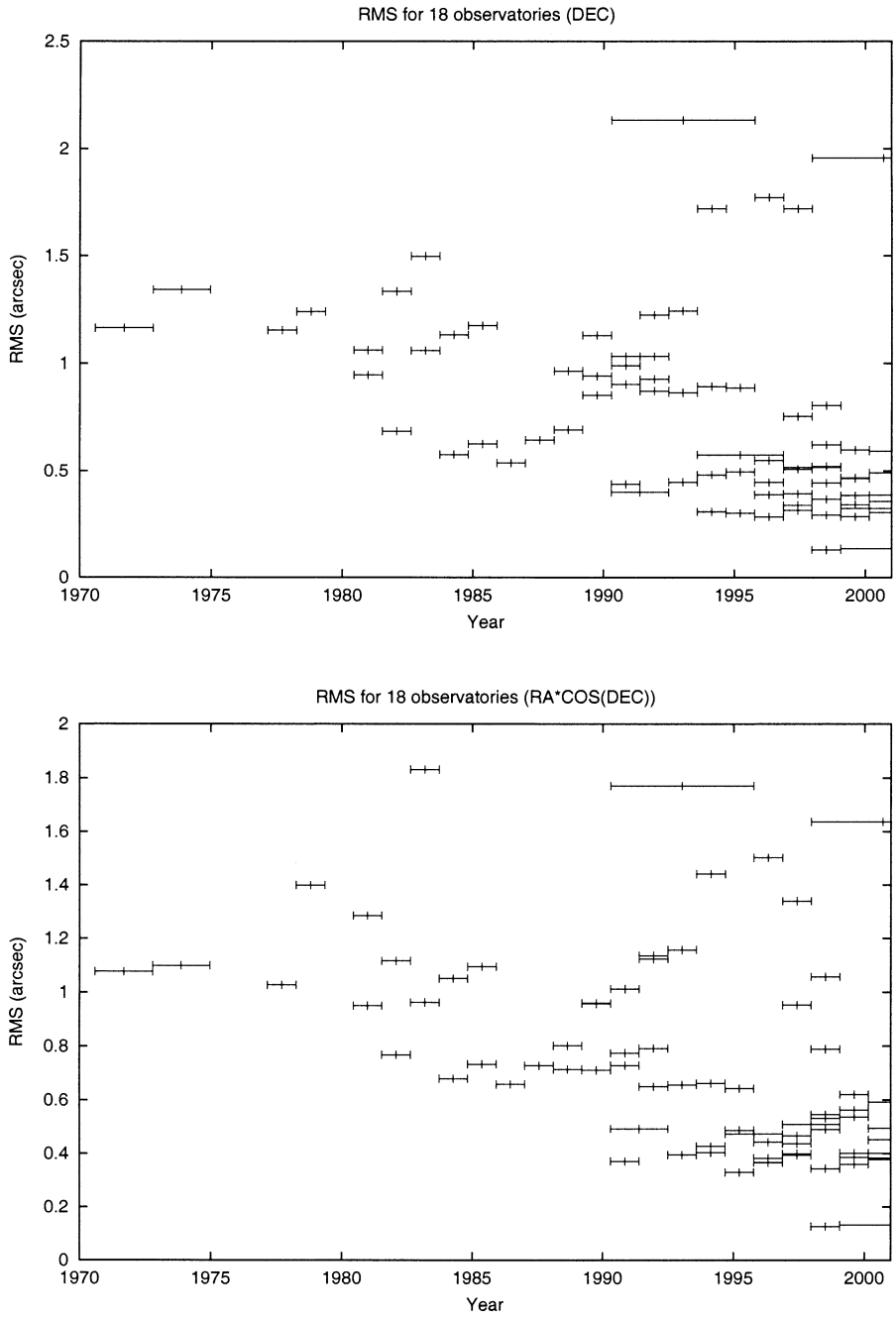

Fig. 4. Time history of the RMS of the residuals in declination (above) and right ascension (below) for the data bins tabulated in Tables 1 and 2, i.e., the bins containing at least 3000 observations. The length of the bars indicates the duration of the bin; thus, a long bar indicates a period of lower productivity.

homogeneous bin, and N_B is the total number of couples contained in B.

The question is how to select the sets of couples, that is B. The values of the correlations are found to be small between observations taken from different observatories (on the order of 1% or less). Thus we have mostly investigated the correlations between the observations of the same observatory. These can be subdivided into subsets either by time difference or by difference in apparent position. The first type of correlation is called *time-wise*, and it appears as a function of the time difference between the observations. It can be expected that the time-wise correlation decreases with time, until it goes to zero or becomes negative; the length of the time difference for which the correlation goes to zero provides important information. The second type is the *space-wise* correlation, which appears as a function of the angular separation on the celestial sphere. We are computing the space-wise correlation by angular difference in an inertial reference frame, looking for effects related to the star catalogs used in the astrometric reductions; there are smaller, but still measurable, effects depending upon the topocentric azimuth and elevation.

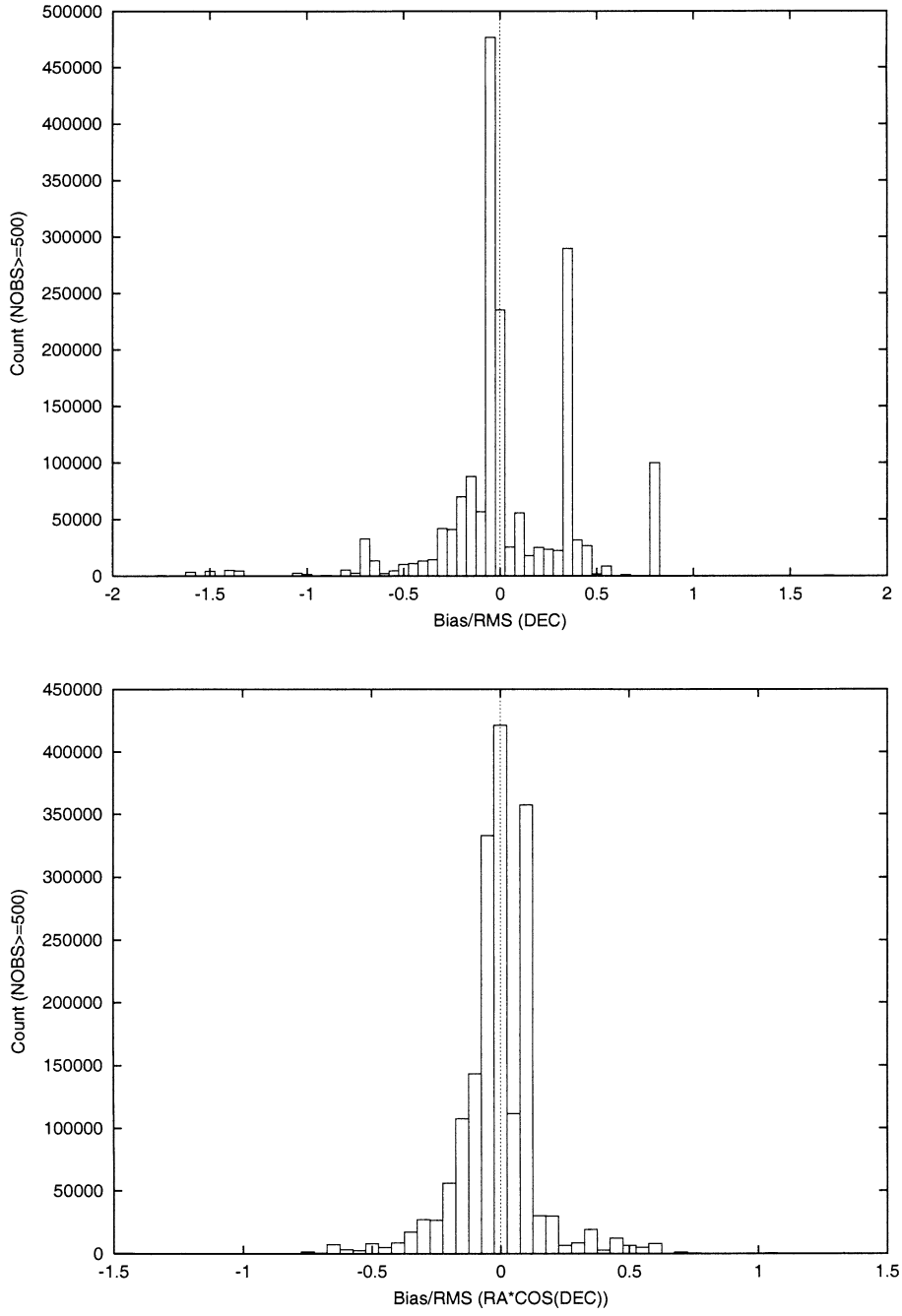

Fig. 5. Histograms of the ratio bias/RMS in declination (above) and right ascension (below). Only data from the 77 largest data bins, which are tabulated in Tables 1 and 2, are included. All observations in each bin (see Section 2) are plotted with the bias/RMS ratio computed for their bin.

We have used for this analysis the same data set described in Section 2. Because the correlation analysis requires large data sets, we have been using the data independently from their partition in data taken with different technologies or reported with different accuracies, but we have not incorporated the observations marked as degraded accuracy by the MPC. Most of the differences between the data from the same observatory are due to changes in equipment and procedures with time; thus, these changes should not degrade the estimation of the short-term time-wise correlations.

4.1. Time-wise correlation

We have selected for this analysis the eight observatory codes with more than 50,000 observations; they have performed 65% of the available observations of numbered asteroids. We have also analyzed two observatories with fewer, but especially accurate observations (transit circles). For each observatory we have computed the correlation of the residuals as a function of time, both for the same asteroid and for different asteroids. In order to show both short-term and long-term effects we have computed the correlations us-

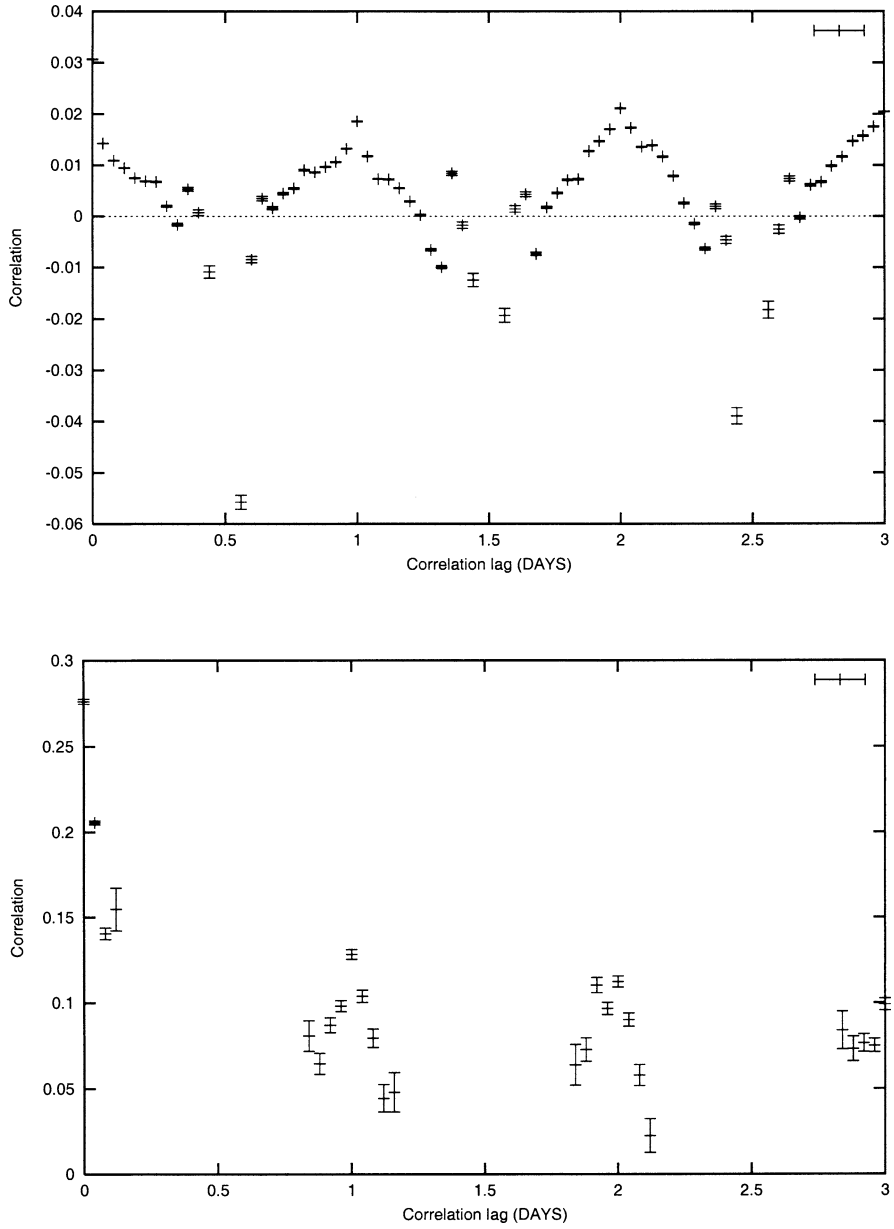

Fig. 6. Time-wise correlation for the right ascension residuals from LINEAR for observations belonging to different asteroids (above) and to the same asteroid (below). In these and in the following plots the empirical correlation points are shown with error bars equal to their formal error $N_B^{-1/2}$, where N_B is the number of couples of observations used for the computation of each point (see Eq. (10)).

ing two different binnings: a short bin of 0.04 d ($\simeq$ 1 h) and a long bin of 1 d. The plots and the fits are obtained from a mixed data set obtained by using the short bin estimate up to the point where its intrinsic error becomes too large due to the small number of observation couples available and the long bin estimate after that point (the value of the time lag at which the transition occurs depends on the observatory considered).

As an example, Fig. 6 shows the correlation in the right ascension residuals as a function of the time difference (or correlation lag) of the observations for LINEAR (observatory code 704). The correlations between observations of the same asteroid (lower half of the figure) show a comparatively high value ($\simeq$ 0.28) for the correlations within the same night, decaying rapidly, and a more slowly decaying component starting from 0.1 for the next night. The gaps in the data correspond to daylight.

The data plotted in the upper half of the figure are the correlations for observations of different asteroids which measure other systematic effects, depending upon time but not upon the portion of the sky which appears in the same frame as the asteroid and thus, we presume, not related with the errors in the star catalogs. These effects are significantly smaller than those affecting the observations of the same asteroid, but are still measurable. The figure clearly shows a signature depending upon the difference in the hour of obser-

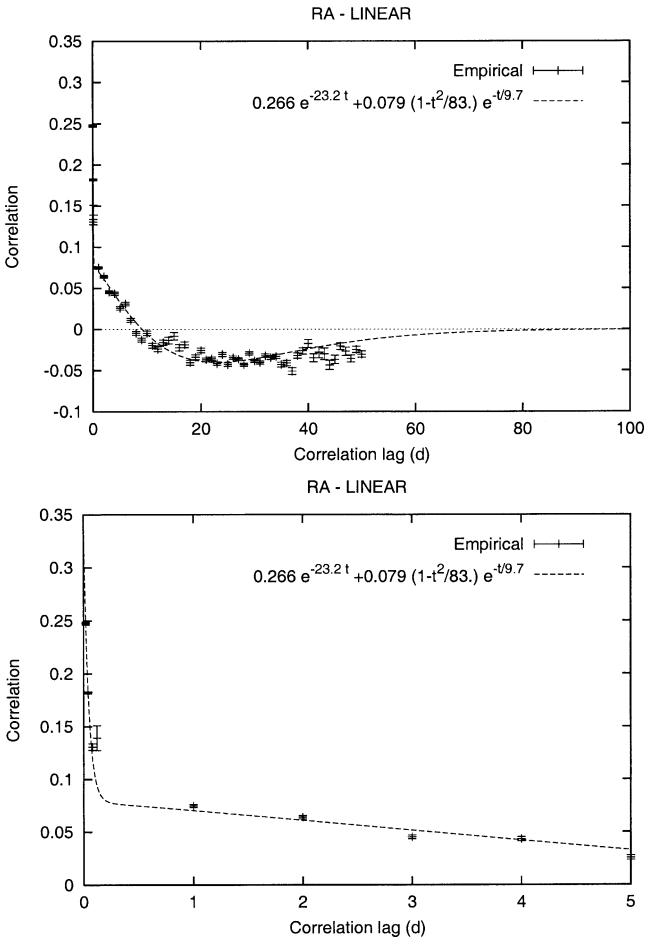

Fig. 7. Correlation among LINEAR right ascension residuals as a function of the time separation between observations of the same asteroid. The computed correlations are depicted as well as the derived correlation function.

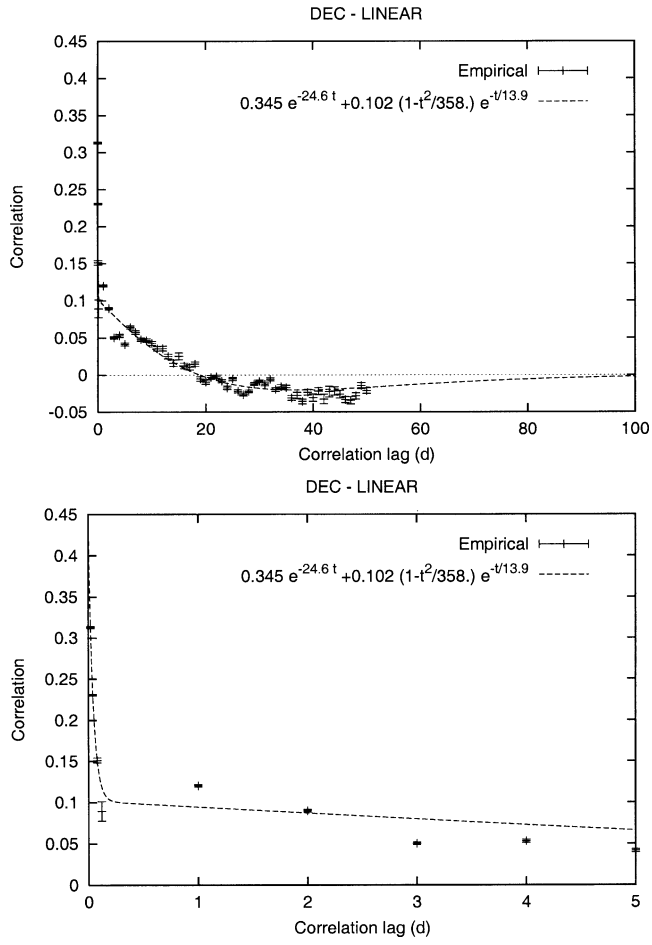

Fig. 8. Same as Fig. 7, but showing the declination results for LINEAR.

vation. This diurnal signature is likely a result of differential refraction, high air mass, increased sky brightness, or some other effect having to do with the elevation of the telescope pointing, all of which would tend to correlate the observational errors.

In Figs. 7 and 8 we show the correlation over two different time spans. Note that the data for correlation lag less than one half day have been binned at a few hours and the rest at integer days. This averages out the effects depending upon the hour of the observations, seen in Fig. 6. The most noteworthy signature of the correlation is that over the time span 20–40 days it becomes negative. The cause of this negative correlation is not clear, but it appears to be a feature of this station, although it is visible in some others. One possible interpretation is discussed in Section 5.

As another example we have chosen the second most prolific survey, LONEOS, which is operated by Lowell observatory at a geographic location not very far from LINEAR. LONEOS uses a different optical system (Schmidt) and different motion-detection algorithms, but is also a highly automated system, hence its large production of observations. Figures 9 and 10 show the correlation in the right ascension and declination residuals as a function of the time difference. The same features of the previous example are apparent, including an even higher peak (> 0.4) at a few hours and a slowly decaying component. Negative correlations do not occur in a systematic way and are likely only the result of somewhat more noisy data (the number of data points being smaller).

We use these figures as examples to illustrate how such information could be used. On one hand, we can make conjectures on the physical or data processing phenomena responsible for each feature visible in the correlation plots. For example, we can presume that the medium-term (1 to 10 days) correlation for the same asteroid is due to systematic, regional errors in the positions of the stars as reported in the star catalog used for the astrometric reductions. The very short term correlation could be due to both the systematic and the random errors in the star catalog: the observations may have been reduced with exactly the same reference stars if the two frames were taken with the same field of view.

On the other hand, it is simply not our job to find out if these conjectures are true. The observers themselves can decide if the systematic effects, which are revealed in the correlations, can be explained and possibly, if they are important enough, removed or compensated for in the data processing.

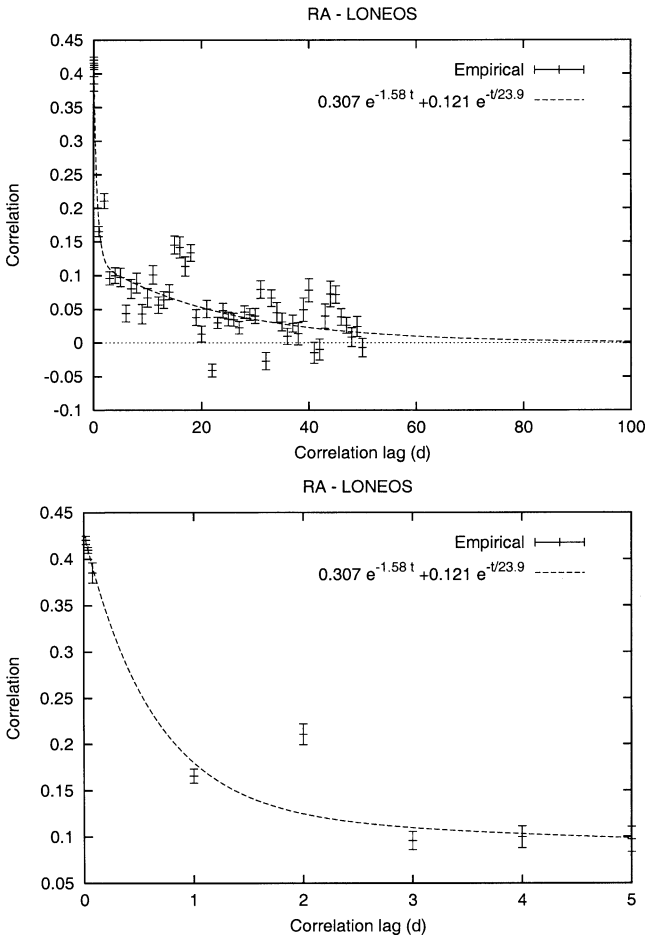

Fig. 9. Same as Fig. 7, but showing the right ascension results for LONEOS.

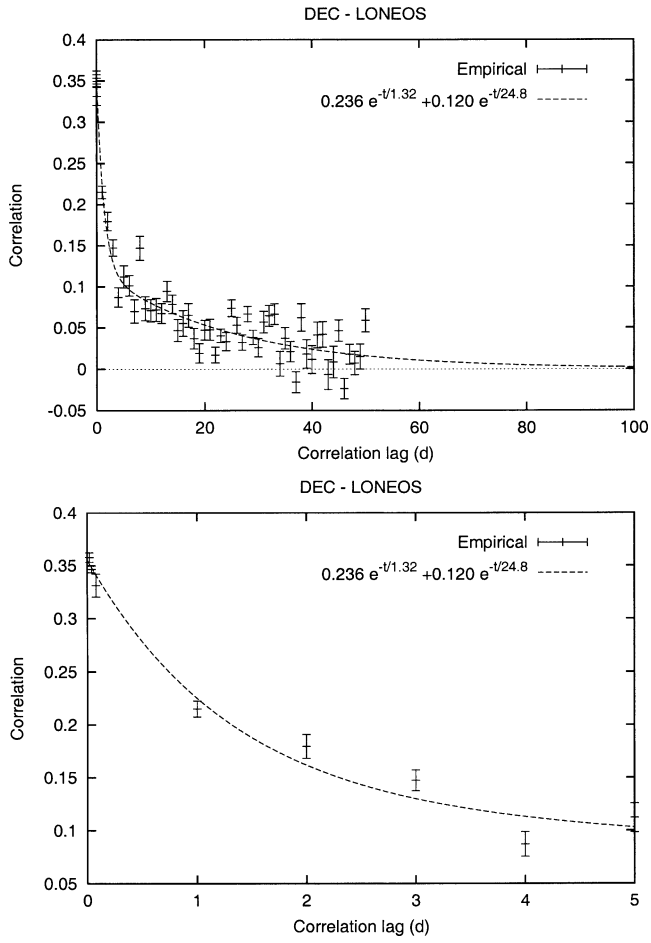

Fig. 10. Same as Fig. 7, but showing the declination results for LONEOS.

From this point of view, our work could be considered as a service to the observers, which might help them in improving their data, if they wish to do so. To make this service available to as many observatories as possible, we are placing online all the figures of this type we have produced. They can be accessed from the home page of each observatory in the information system AstDyS.

However, the main purpose of our analysis of correlation is not to explain it, but to define an a posteriori model for it. Such a model can be used to fit the data as they are, without degrading the quality of the orbits thus determined and the reliability of the confidence regions computed on the basis of the corresponding covariance matrices. This is the subject of the next section.

4.2. Correlated weighting

This paper has the purpose of developing a sound observation error model, and the way in which this model will be used in future, e.g., for improved orbit determination, is the subject of continuing research. However, we need to anticipate that one of the intended purposes of this work is to define a modified least-square method, in which the target function to be minimized will be expressed, as a function of the vector of residuals $\Xi = [\xi_i]$, as

$$Q = \frac{1}{m} \sum_{i,j=1}^{m} \xi_i w_{ij} \xi_j = \frac{1}{m} \Xi \cdot W \Xi, \tag{11}$$

where the weight matrix $W = w_{ij}$ is not a diagonal matrix.

To maintain the same formalism, and the same probabilistic interpretation based upon the Gaussian probability densities of the classical least-square method, the only requirement is that the weight matrix W is the inverse of the covariance matrix $\Gamma = [\gamma_{ij}]$ of the observations. In the traditional, uncorrelated models for observation errors the matrix is zero apart from the diagonal elements $w_{ii} = 1/\sigma_i^2$, where σ_i^2 is the variance (and σ_i the RMS) of the assumed Gaussian error probability distribution for residual ξ_i. On the contrary, if the residuals ξ_i and ξ_j contain observation errors with RMS σ_i and σ_j, respectively, and with correlation r_{ij}, the covariance matrix Γ should have elements

$$\gamma_{ij} = r_{ij} \sigma_i \sigma_j . \tag{12}$$

Of course, the inversion $W = \Gamma^{-1}$ could become difficult to handle computationally if the matrix Γ were full, but this is not the case if we assume that only the observations from the same observatory are correlated. In fact, the time correlations decay with time, and most systematic effects (apart

from those accounted by the biases) should not result in significant correlations between observations performed at different oppositions. (We have to acknowledge that this is an assumption, which is very difficult to be tested empirically with the data.) Thus we can decompose the vector Ξ into blocks Ξ_α corresponding to observations by the same observatory during the same opposition; the index α designates one *passage* of an asteroid in the field of view of one observatory, during the nearby nights of one apparition (this terminology is taken from artificial satellite orbit determination, where the meaning is more intuitive). The matrix Γ is then decomposed into square blocks Γ_α, one for each passage, of moderate size, and they can be easily inverted: $W_\alpha = \Gamma_\alpha^{-1}$. Then the matrix W is known, and indeed the computations involving the target function Q and its derivatives can be performed passage by passage, that is block by block, e.g.:

$$Q = \frac{1}{m} \sum_\alpha \Xi_\alpha \cdot W_\alpha \Xi_\alpha. \tag{13}$$

Note that this approach is correct only if we can neglect the correlations between observations at different oppositions, that is, if the time correlation goes to zero with increasing time and is practically negligible for times longer than a few months. Thus the biases have to be removed: if there were biases left in the observation errors, they would result in non-decaying time correlations. In other words, if $B = [b_i]$ is the vector of biases b_i for each residual ξ_i the target function actually is

$$\begin{aligned} Q &= \frac{1}{m} \sum_{i,j=1}^{m} (\xi_i - b_i) w_{ij} (\xi_j - b_j) \\ &= \frac{1}{m} (\Xi - B) \cdot W (\Xi - B). \end{aligned} \tag{14}$$

We have described in Section 3 how to estimate RMS and biases for the individual observations. To make the correlated least-square algorithm possible we need to be able to compute the correlation r_{ij} for each couple of observations, taken by the same station s at times t_i and t_j, respectively. (We can assume the times are not more than few months apart.) The idea is to use an a priori estimation of the correlation of the form

$$r_{ij} = R_s(T) \tag{15}$$

with R_s a function of the time difference $T = |t_j - t_i|$; the functions are different for different observatories (also different for right ascension and declination).

Thus the goal of the time-wise correlation analysis should be to find the most suitable time-correlation functions R_s for each station. In practice, this estimation can be performed only for the stations with the most data, because for low production stations the scatter of values for the estimated correlation would be too large due to small number statistics in each time bin. We have computed best-fitting time-correlation functions for the eight stations with the most data (more than 50,000 observations each), which comprise two thirds of the data set. We have also computed the time-correlation functions for two especially accurate transit circles. The results for these 10 stations are summarized in Table 3.

In Figs. 7–10 the best-fitting time-correlation function is represented by a dashed line. It is apparent that such a synthetic time-correlation function can represent the main features of the actual time-wise correlation contained in the data, but not all the details. We have decided, for example, to ignore the diurnal effect by which the correlation function should oscillate with period one day (thus we have used one day bins beyond the first night).

In determining the best-fitting correlation functions, it is not the case that we can use a linear combination of an arbitrary set of functions. There are conditions to be satisfied to ensure that the covariance matrix Γ_α is always positive definite. It can be shown (Mussio, 1984) that only certain functions of time have the property of ensuring that the correlation matrix $R = [r_{ij}]$ defined by Eq. (15) is positive definite, so that also the covariance matrix defined by Eq. (12) is positive definite. One requirement is that all of these functions must decay to zero with time: $\lim_{T\to+\infty} R_s(T) = 0$. The list of such functions include decaying exponential $\exp(-cT)$ and Gaussian functions $\exp(-cT^2)$, and also quadratic times exponential functions of the form $(1 - dT^2)\exp(-cT^2)$ and all their linear combinations. For each station, and separately for right ascension and declination, we select some of these functions $f_k(T)$ (in practice, we have used either one or two, possibly including two exponential functions with very different values of the exponent coefficient c_k); then we perform a least-square fit of the combination $\sum z_k f_k(T)$ to obtain the values of the coefficients c_k, d_k contained in the functions and of the linear coefficients z_k. Note that this fit is nonlinear in the coefficients c_k, d_k; thus some reasonable initial guess is required. At present, a this procedure is not automated.

We believe that we have found, by means of the time-correlation functions of Table 3, a good approximate representation for most of the correlation present in the real data set. This, however, leaves a problem: if the time-correlation function is very different from one station to another, what should we do with the observations from observatories with not enough data to compute such a function? To use these data without taking into account the correlations would amount to inappropriately overweighting them with respect to the data of the stations for which correlation is taken into account in the weight matrix. We have found a compromise solution, consisting in the computation of a time-correlation function with mixed data, coming from all the other observatories except those 10 listed in the table. We use the label "MIX" to refer to this mixed set of observatories. Figures 11 and 12 show the actual time-wise correlation, obtained by computing a correlation only among data of the same observatory but then averaging the results over all the observatories except the 10 of the table. These figures also show the

Table 3
Fitted models of correlation functions for 10 major observatories

Observatory	Right ascension	Declination
095	$0.248e^{-0.0251T}$	$0.299e^{-0.0199T}$
675	$0.266\left(1-0.0349T^2\right)e^{-0.225T}$	$0.398e^{-0.176T}$
689[a]	$0.145e^{-1.11^T}+0.146e^{-0.00151T}$	$0.193e^{-1.29T}+0.129e^{-0.00674T}$
691	$0.815\mathrm{e}^{-8.36T}$	$0.453e^{-24.6T}+0.373e^{-0.126T}$
699	$0.307e^{-1.58T}+0.121e^{-0.0418T}$	$0.236e^{-0.760T}+0.120e^{-0.0403T}$
703	$0.179e^{-0.0445T}$	$0.176e^{-0.0373T}$
704	$0.266e^{-23.2T}+0.079\left(1-0.0121T^2\right)e^{-0.103T}$	$0.345e^{-24.6T}+0.102\left(1-0.00279T^2\right)e^{-0.0717T}$
809	$0.470e^{-28.9T}+0.312\left(1-0.0361T^2\right)e^{-0.240T}$	$0.394e^{-17.6T}+0.422e^{-0.258T}$
950[a]	$0.205\left(1-0.000630T^2\right)e^{-0.000445T^2}$	$0.051e^{-0.0139T}$
999[a]	$0.145e^{-0.0236T}$	$0.079e^{-0.0139T}$
MIX[b]	$0.246e^{-24.8T}+0.133\left(1-0.00490T^2\right)e^{-0.109T}$	$0.222e^{-1.42T}+0.106e^{-0.00459T^2}$

Note. Refer to Table 2 for the names corresponding to most of the observatories in this table. Additionally, code 950 denotes La Palma and 999 denotes Bordeaux-Floirac.

[a] Correlation functions are usually computed by taking into account only observations having a residual RMS lower or equal to 3 arcsec (both in RA and DEC), which are generally reported by the MPC to 0.01 s in RA and 0.1 arcsec in DEC. However, for observatories 689, 950 and 999, where transit circles are located, only the observations reported by the MPC to 0.001 s in RA and 0.01 arcsec in DEC are included; these amount to 89.3% of the total number of observations for observatory 689, 98.7% for 950, and 63.8% for 999.

[b] The MIX class corresponds to observations belonging to all the other observatories. It is computed by taking into account only observations for which a specific RMS value has been obtained. Note that only correlations between observations from the same site are computed; however, to compensate for the small number statistics, these correlations for time bins from different observatories are fitted together to a single time-correlation function (see Figs. 11 and 12).

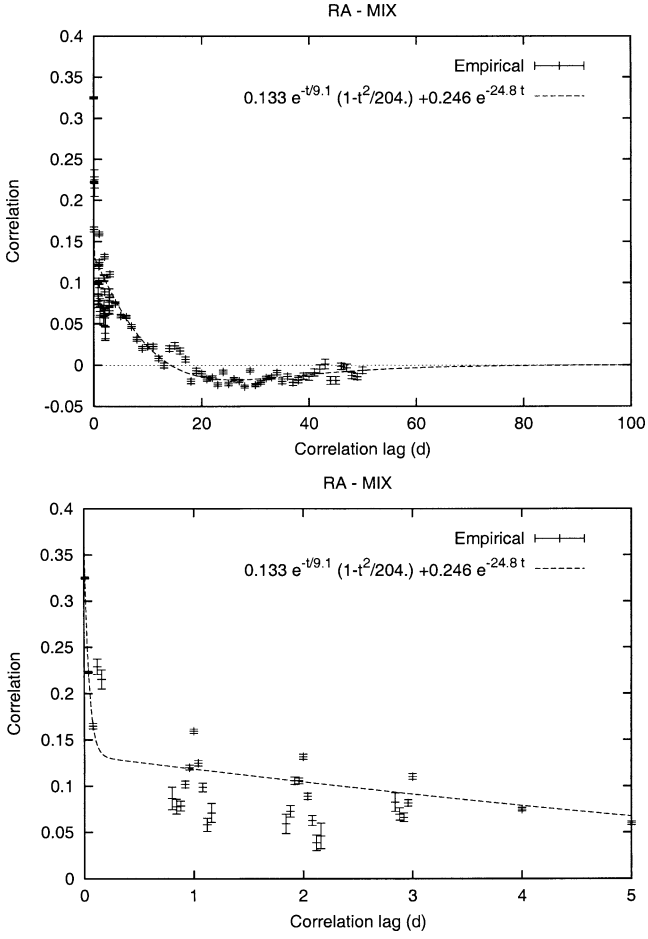

Fig. 11. Same as Fig. 7, but showing the right ascension results for the MIX group of observatories.

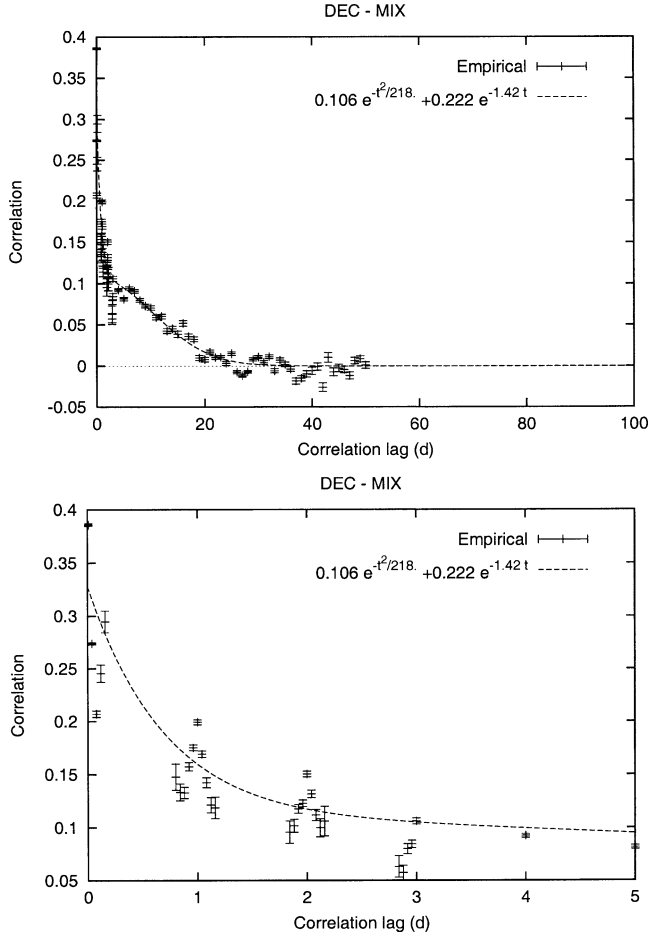

Fig. 12. Same as Fig. 7, but showing the declination results for the MIX group of observatories.

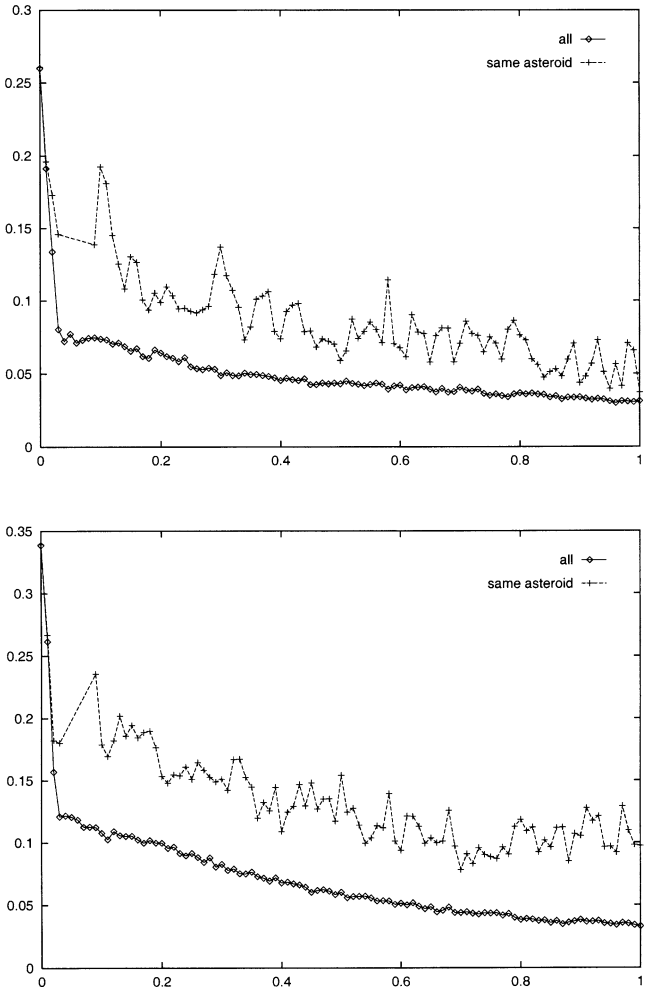

Fig. 13. Correlations in the right ascension residuals (above) and declination residuals (below), as a function of the angular separation on the celestial sphere (in degrees), between observations of the same asteroid (upper line, dashed) and between all observations (lower curve, continuous), for the data set of all the numbered asteroids observed by LINEAR.

best-fitting function as a dashed line. The results are, as it should be expected, not very accurate models of the actual correlations for a specific observatory, but significantly better than ignoring the correlations altogether. This inaccuracy is not a source of great concern, because the lower production observatories are not the automatic surveys, and they do not normally observe the same asteroid many times per night. Thus the MIX time-correlation function will be used much less than the others in future correlated least-squares orbital solutions.

4.3. Space-wise correlation

We have conjectured that a significant cause of the correlations between observations of the same asteroid with a short time difference is due to the systematic errors contained in the star catalogs. This hypothesis can be confirmed by looking at the space-wise correlation of the residuals.

Figure 13 shows the correlation of the residuals as a function of angular distance on the celestial sphere. We have used for this purpose the large and comparatively homogeneous data set of 813,822 observations of numbered asteroids from the LINEAR survey (observatory code 704).

For very low angular distance (< 0.03 degrees) the correlation between all the observations is dominated by the correlation between observations of the same asteroid, for the obvious reason that there are few cases in which two different asteroids are seen within the same small patch. For larger angular separations the couples formed by different asteroids are by far more numerous, and their correlation is not insignificant, in the range between 0.12 and 0.03. This could be interpreted as the effect of systematic errors in the star catalog used in the LINEAR astrometric reductions, which affect all asteroids which happen to be imaged against the same background of stars.

The correlations of the subset of couples formed by observations of the same asteroid are anyway larger, although the curve is more noisy due to the much smaller sample. This is related to the time-wise correlation: in comparing Fig. 13 with Fig. 6 we need to take into account that the average proper motion of a main belt asteroid is 0.2 degrees per day. The values of the correlations and for time intervals of 1, 2, and 3 days are to a good approximation the same as the correlations for angular distances of 0.2, 0.4, 0.6 degrees, respectively. The question arises whether these correlations are better described as space-wise rather than time-wise correlations. The only way to discriminate is to analyze separately asteroids with very different proper motion, e.g., main belt and NEA. We plan to address this question in the future.

The space-wise correlation can be analyzed, when the data set is large enough, by adding to the control on angular difference some control on time difference, e.g., space-wise correlation only for data taken within a time difference of a few years. This could give better information on the effect of star catalogs changing over the years. We have not performed this analysis for the LINEAR data because they are all recent.

Thus the correlations between observations of the same asteroid, as well as the peak in spatial correlations for angular distances < 0.03 degrees, can be handled by the method we have outlined to take into account the time-wise correlation. The remaining tail of correlation between different asteroids can be understood only as the effect of systematic star catalog errors. There is no computationally efficient way to account for this effect in the orbit determination process, because it would require us to solve for all the orbits of all asteroids at once, with a normal matrix which is not block diagonal.

The effect of star catalog errors can be decreased, for the future, by the use of the more accurate star catalogs now available as a result of, for example, the ESA Hipparcos mission. Even for the observations already contained in the data archives, some a posteriori corrections could improve the quality of the data if the MPC were to make available,

in a format suitable for the orbit computers, the information supplied with the observations submission form on the star catalog used in the reduction. (This should indeed happen when the new observation format is implemented by the MPC.) Both global rotations and zonal corrections can be applied to align the reductions performed with old star catalogs, on average, with the current ICRS reference system. This can result in improvements which are small in size but important because they affect very large data sets.

5. Conclusions

5.1. Tasks completed

We would like to assess the degree to which we have achieved the goal of confirming the existence of a Gaussian statistical error model for the asteroid optical astrometric observations. Overall, we believe we have achieved this goal, albeit with the following caveats and limitations:

1. The observation errors can follow a Gaussian statistic only after outlier removal. By examining the distribution of the residuals which are not removed (e.g., in Fig. 3) we find that the tail of the distribution at large residuals (beyond $\sqrt{8}$ times the RMS) has been removed. If the distribution was indeed the sum of a perfect Gaussian of "good" data and of a distribution of "bad" outliers, then our outlier removal algorithm (described in Section 2) would have thrown away a small number of "good" data along with the "bad." However, the use of a probability density for the errors which is always positive, even for very large errors, is not based upon any compelling reasons having to do with the nature of the measurement process. It was indeed the opinion of Gauss (1809, p. 254) that a probability density with compact support would be more appropriate, the use of analytic functions (in particular, of exponentials) being dictated by the possibility of using more elegant mathematical arguments.
2. There are some unusual signatures in the results, such as the pointed non-Gaussian shape of the distribution of LINEAR residuals (Fig. 3) and the negative time-correlations of LINEAR residuals (Fig. 7). We can conjecture that these are the result of the overweighting of the data from what is by far the most prolific observing site. The overweighting would naturally result from neglecting the correlations, which are more important in this case because of the standard procedure used by LINEAR, involving an automated sequence of five observations within a few hours. This conjecture can be tested by redoing the same plot after applying the correlated weighting proposed in Section 4.2.
3. The error model, which we have obtained by analyzing the residuals, unlike all the a priori models used so far (at least in the processing of asteroid astrometry), is not a simple one, with uncorrelated, unbiased Gaussian distributions. The hypersurfaces, which play the role of level manifolds for the target function Q and also of level manifolds for the probability density of the errors, are simple, symmetric spheres (centered on the origin) for the most basic least-square principle, in which the target function is exactly a sum of squares. The spheres have been replaced by ellipsoids with uneven axes not aligned with the coordinate axes, and with center not in the origin. This should not be surprising: every level manifold of a function near its maximum is well approximated by some ellipsoid, whose equation is obtained by truncating the Taylor expansion to degree two. There is no reason why such ellipsoids should in particular be spheres.
4. We have not used all the possible information to form homogeneous bins of data, for the purpose of computing RMS and biases. More work may be possible in the future on the influence of proper motion, apparent magnitude, and star catalog selection on the accuracy of the observations.

The next issue is whether we have achieved the task of finding the most appropriate parameters for such a Gaussian error model. The answer is again that we have obtained a solution for these parameters, which is rigorously founded on the analysis of a large set of data, with the following caveats:

1. The RMS and especially the biases are not very reliable for observatories and time intervals with low data production rate.
2. The time-wise correlations have been modeled for the most productive stations, for the other stations the mixed correlation function is a rougher approximation.
3. Space-wise correlations and local time effects have not been handled; we believe they are second order effects, but this should be checked.

This model by itself is useful to assess the performance of the different observatories (and its evolution with time); the observers may even be able to take corrective action if they want to. If this happens, the observers are requested to inform us, to allow for an appropriate update of the error model.

5.2. Future work

We conclude by summarizing the work which remains to be done to achieve our third goal, namely improving the orbit determination (and all its consequences) by the systematic application of this error model in the processing of the astrometric observations.

1. We need to implement in software the weighting scheme described in Section 4.2, with weights and biases based upon station performance and correlations based on our empirical time-correlation functions. Then we can ex-

periment with the generation of large orbit catalogs, including a new global solution for all numbered asteroids.
2. We need to reanalyze the residuals after applying the more advanced weighting scheme and see how large the changes are to the parameters used in the error model itself. The procedure is in fact an iterative one; we may need to significantly change the model after the first iteration is complete.
3. We would like to know if, after the first iteration, there are changes in the non-Gaussian signatures. As an example, both the negative time-correlations and the pointed distributions can be interpreted as the consequences of overweighting of some very large production observatories. The new scheme should provide a more balanced weighting; thus some orbital errors resulting from overweighting could go away, and the residuals should represent in a more pure way the observation errors, which could be more precisely Gaussian.
4. The main issue, however, is not the internal consistency of the theory, that is, the accuracy with which a Gaussian model fits the data. Rather, the real goal is to improve the external consistency of the theory with the real world. In other words, we want to compute orbits more adherent to the reality of the asteroid true trajectories and covariance matrices more accurately representing the range of values possible for the orbital parameters (and their consequences, such as future observations and close approaches). This can be tested by computing predictions of observations and orbit identifications by using different weighting schemes and then by checking if independent sources of information (e.g., additional observations not used in the fit) better confirm the predictions based upon a more advanced weighting scheme.
5. The availability of radar astrometry is a good external test since the weights for radar range and range-rate measurements are computed by an entirely different method, one based on the way the individual radar signals are combined into astrometry. The quality of the fits and of the resulting predictions would depend upon an appropriate relative weighting between radar and optical data.

The above program of research will be pursued in the near future by the authors of the present paper, in collaboration with other authors.

Acknowledgments

We have discussed the subject of this paper with many colleagues, and in particular we thank P. Chodas, M.E. Sansaturio, S. Ostro, E. Bowell, K. Muinonen, and F. Sansò for contributing relevant comments; we are also grateful for the suggestions given by the two referees (T.B. Spahr and an anonymous referee) of the preliminary version of the paper. We thank all the observers producing asteroid astrometry because their work is what this paper is all about, and we particularly welcome their comments and suggestions. The work described in this paper was completed at the Astronomical Observatory of Milan/Brera and at the University of Pisa, under contracts with the Italian Space Agency (ASI), the Spanish *Ministerio de Ciencia y Tecnologia* and with European funds *FEDER* through Grant AYA2001-1784, and at the Jet Propulsion Laboratory, California Institute of Technology, under a contract with the National Aeronautics and Space Administration. The OrbFit free software system is maintained by a consortium led by A. Milani, M. Carpino, Z. Kneževič, and G.B. Valsecchi; it is available at http://newton.dm.unipi.it/asteroid/orbfit/. The statistical data on the performance of each observatory are provided with the OrbFit distribution, in the ./lib/num*.cl* files. They are also disseminated through the AstDyS online information system (http://hamilton.dm.unipi.it/astdys/ in the home page for each observatory), where the data corresponding to those of Tables 1 and 2, and also the time-wise correlation plots such as those of Figs. 7–12 are published.

References

Cappellari, J.O., Velez, C.E., Fuchs, A.J., 1976. Mathematical Theory of Goddard Trajectory Determination System. Goddard Space Flight Center, Greenbelt, MD.

Danby, J.M.A., 1988. Celestial Mechanics, 2nd edition. Willmann–Bell, Richmond, VA.

Gauss, C.F., 1809. Theory of the Motion of the Heavenly Moving about the Sun in Conic Sections. Reprinted by Dover, New York, 1963.

Milani, A., 1999. The asteroid identification problem I. Recovery of lost asteroids. Icarus 137, 269–292.

Milani, A., Valsecchi, G.B., 1999. The asteroid identification problem II: target plane confidence boundaries. Icarus 140, 408–423.

Milani, A., La Spina, A., Sansaturio, M.E., Chesley, S.R., 2000a. The asteroid identification problem III: proposing identifications. Icarus 144, 39–53.

Milani, A., Chesley, S.R., Valsecchi, G.B., 2000b. Asteroid close encounters with Earth: risk assessment. Planet. Space Sci. 48, 945–954.

Milani, A., Sansaturio, M.E., Chesley, S.R., 2001. The asteroid identification problem IV: attributions. Icarus 151, 150–159.

Mussio, L., 1984. Il metodo della collocazione minimi quadrati e le sue applicazioni per l'analisi statistica dei risultati delle compensazioni. Ric. Geod. Topogra. Fotogram. 4, 305–338.